# *High Energy Emission from Pulsar Magnetospheres*

**HIROTANI, Kouichi**

*ASIAA/TIARA, Taiwan*

**Workshop on BH Magnetospheres**
**Hiroshima University**
**March 2, 2015**

Crab nebula: Composite image of X-ray [blue] and optical [red]

# §1 γ-ray Pulsar Observations

Before 2008, EGRET aboard CGRO had detected 272 point sources above 100 MeV.

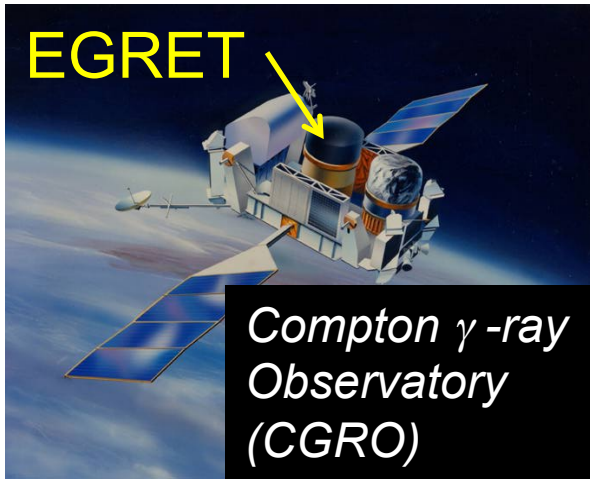


EGRET point sources (>100 MeV)

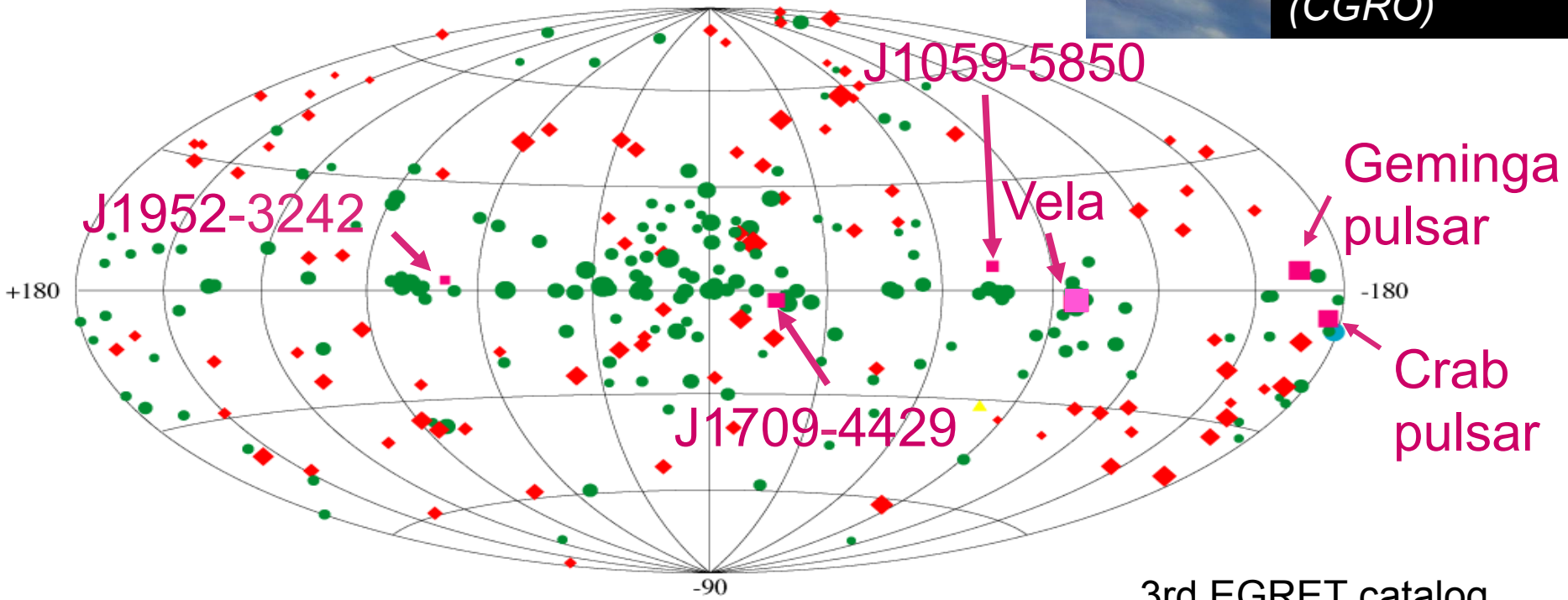


3rd EGRET catalog (Hartman+ 1999)

# §1 γ-ray Pulsar Observations

Before 2008, EGRET detected only 6 pulsars, which distribute along the Milky Way.

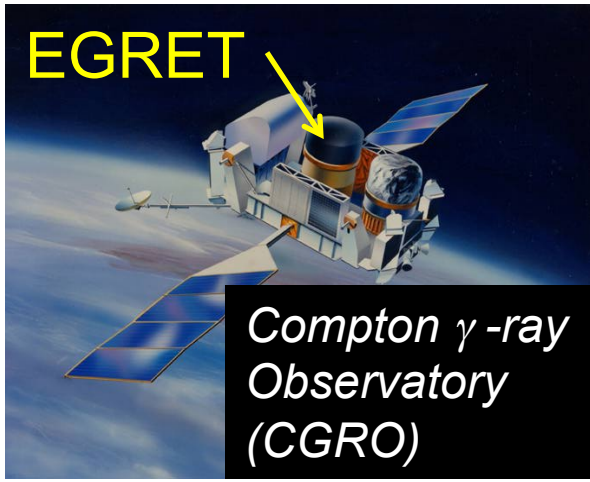


EGRET point sources (>100 MeV)

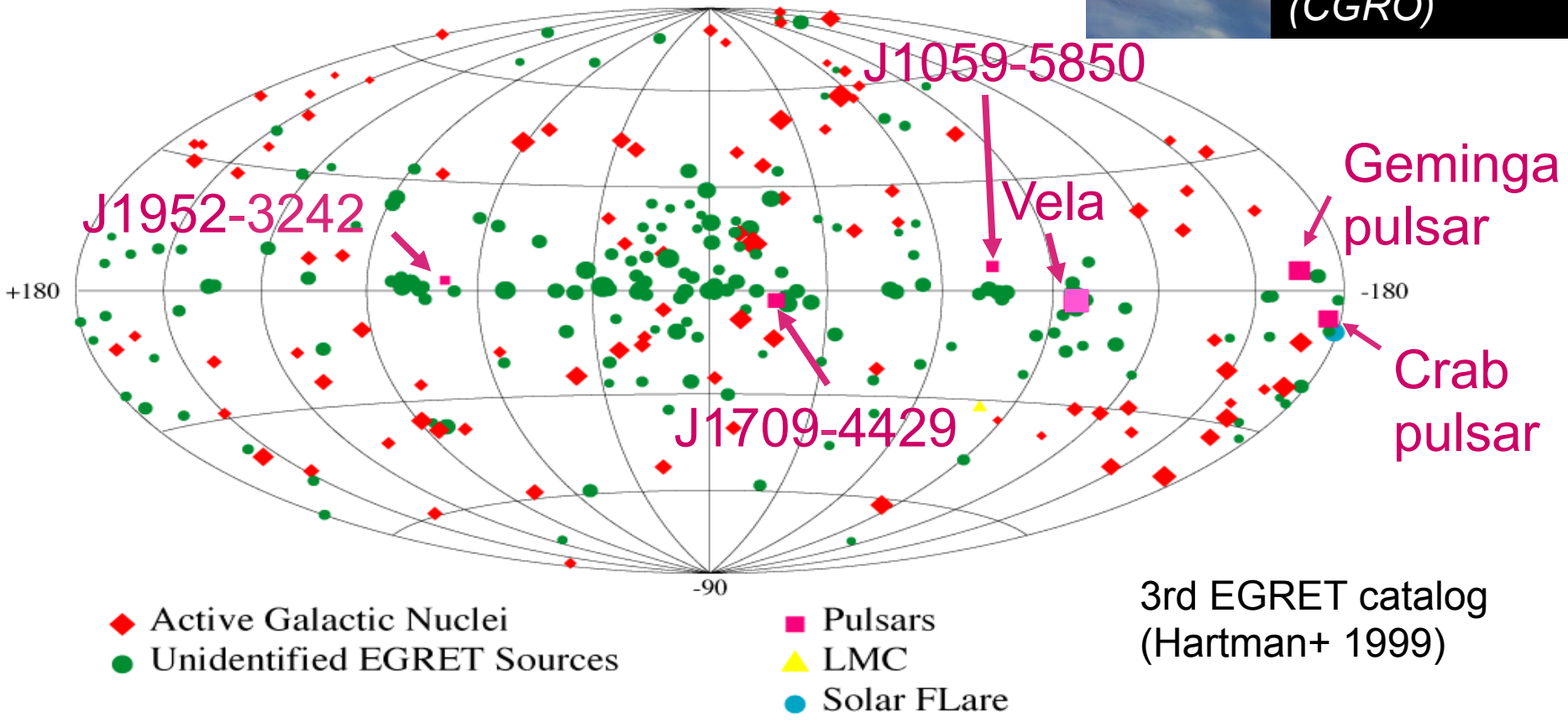


3rd EGRET catalog (Hartman+ 1999)

# §1 γ-ray Pulsar Observations

After 2008, LAT aboard Fermi has detected more than 117 pulsars above 100 MeV.

Large Area Telescope


*Fermi γ-ray space telescope*

Fermi/LAT point sources (>100 MeV)

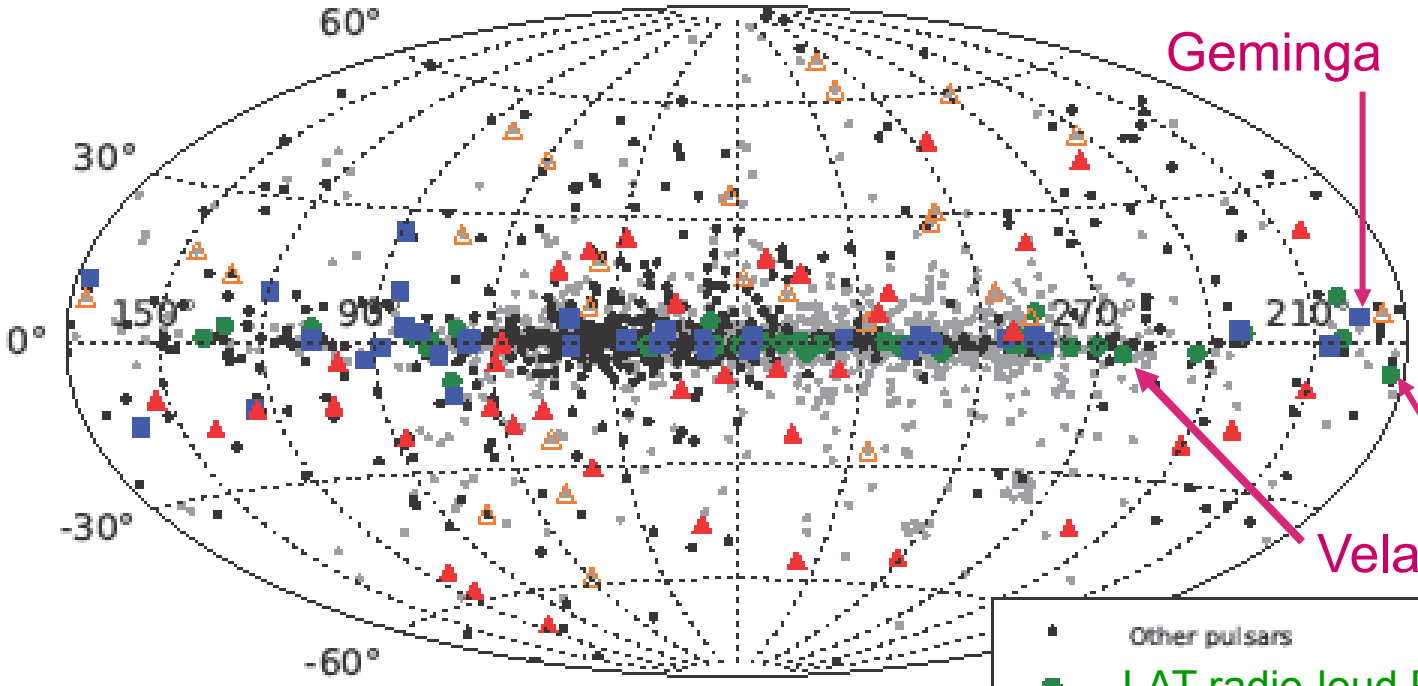


2nd LAT catalog (Abdo+ 2013)

Blazer +other AGN jets (330+58)

# §1 γ-ray Pulsar Observations

In VHE (~TeV), the first detection of pulsed emissions was reported by VERITAS, ground-based, Imaging Air Cherenkov Telescopes (IACTs) from the Crab pulsar.

VERITAS ( > 120 GeV)

Aliu+ (2011, Science 334, 69)

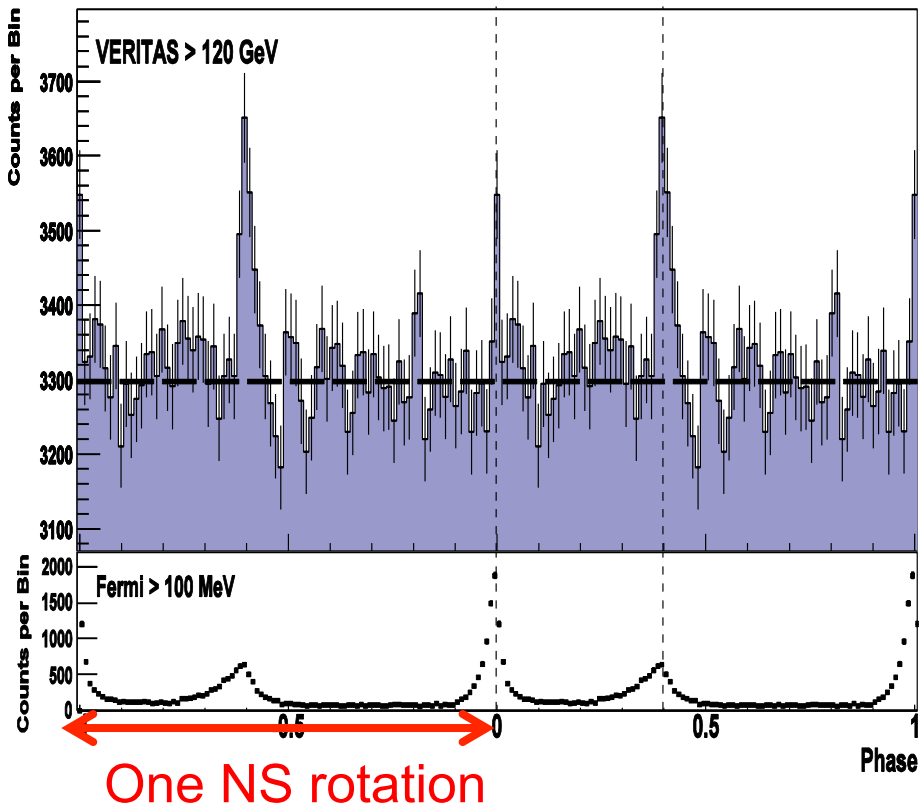


Very Energetic Radiation Imaging Telescope Array System

Arizona, U. S. A.
Four 12m optical reflectors
Sensitive in 50 GeV – 50 TeV

# §1 γ-ray Pulsar Observations

Almost at the same time, MAGIC, another IACTs, reported pulsed signals from Crab above 25 GeV.

MAGIC (25–416 GeV)

Aleksić+ (2011a,b)

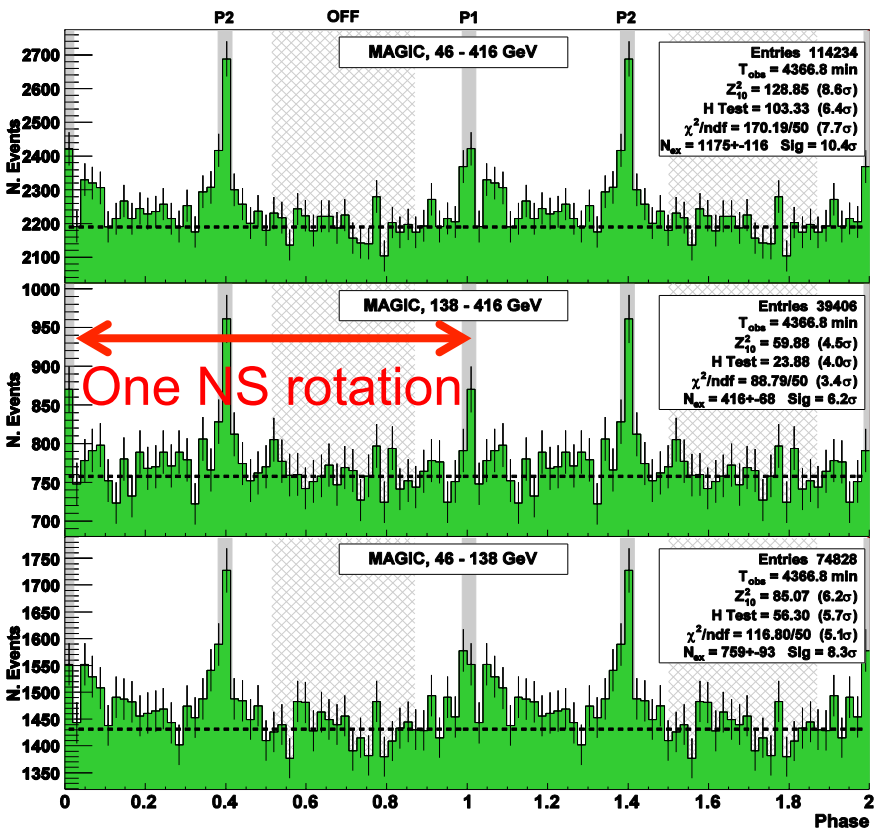


Major Atmospheric Gamma-ray Imaging Cherenkov Telescopes

La Palma, Canary Islands
Two 17m optical reflectors
Sensitive in 25 GeV – 30 TeV

# *Pulsed broad-band spectra of young pulsars*

- High-energy (>100MeV) photons are emitted mainly via **curvature** process by ultra-relativistic, primary $e^-$'s/$e^+$'s.

(created in particle accelerator)

Fermi/LAT
(sensitive in 20 MeV – 300 GeV)

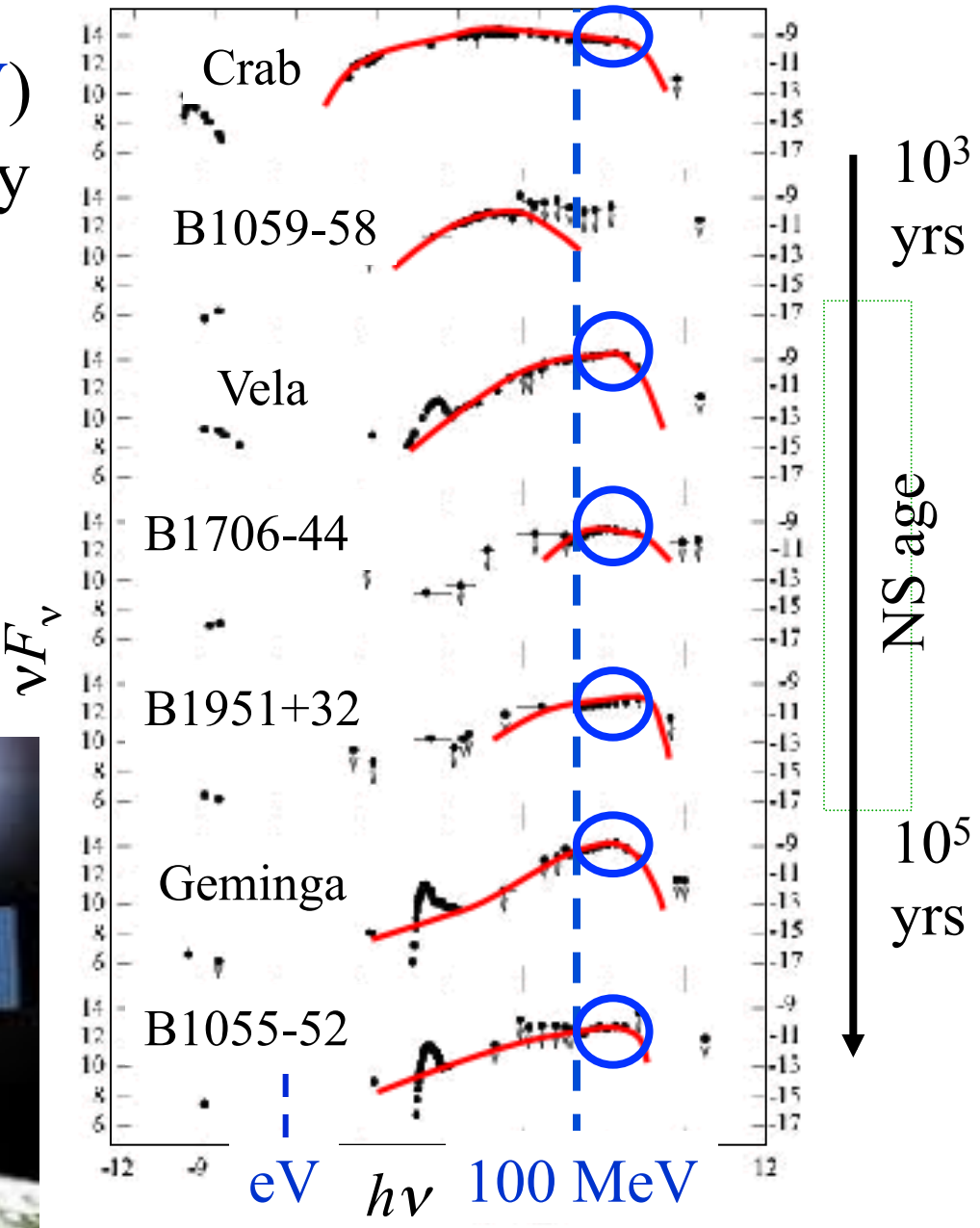

# *Pulsed broad-band spectra of young pulsars*

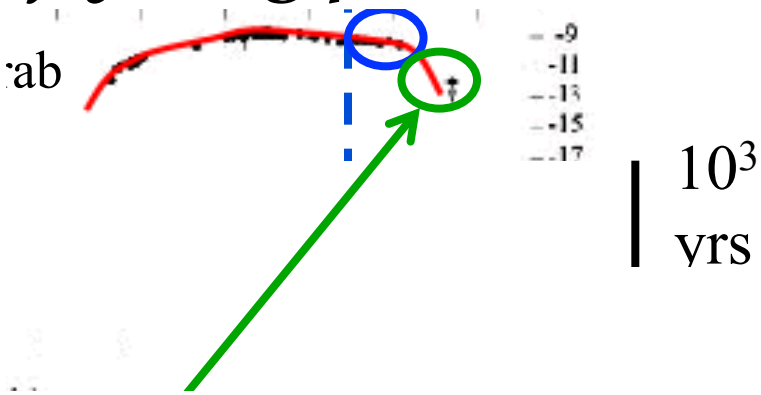


- High-energy (>100 MeV) photons are emitted mainly via **curvature** process by ultra-relativistic $e^{\pm}$'s.

- However, > 20 GeV, **Inverse-Compton scatterings (ICS) by the cascaded $e^{\pm}$'s** contribute.


# *Pulsed broad-band spectra of young pulsars*

- High-energy (> 100MeV) photons are emitted mainly via **curvature** process by ultra-relativistic $e^{\pm}$'s.

- However, > 20 GeV, **ICS by secondary & tertiary pairs** contributes.

- Some of the γ-rays are absorbed in the NS magnetosphere to be reprocessed via **synchrotron** process.

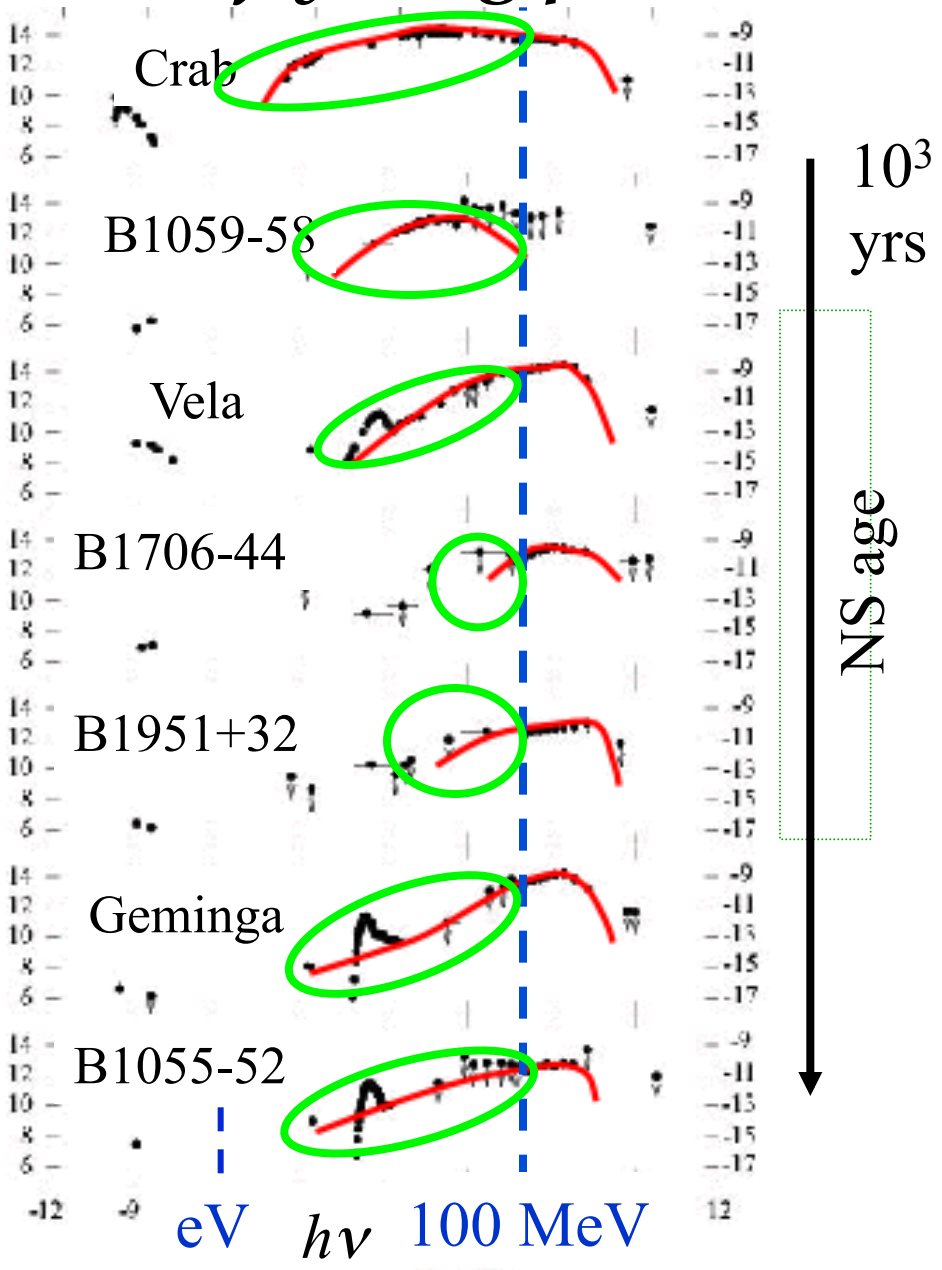

# §2 Pulsar Emission Models

Let consider how and where such incoherent, high-energy photons are emitted from pulsars.

# §2 Pulsar Emission Models

If copious charges are (somehow) supplied, they realize a force-free magnetosphere, $\boldsymbol{E}\cdot\boldsymbol{B}=0$, and corotate with the magnetosphere under the corotational electric field,

$$\boldsymbol{E}_{\perp} \equiv -c^{-1}(\boldsymbol{\Omega}\times\boldsymbol{r})\times\boldsymbol{B}.$$

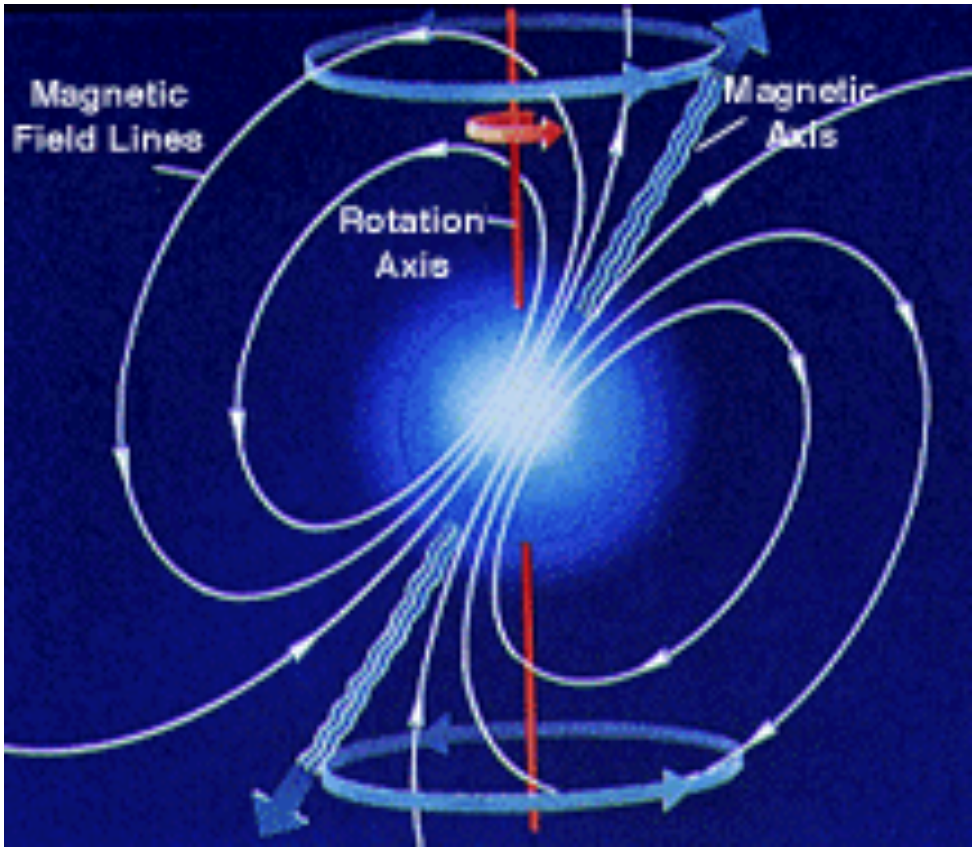


Charges corotate by $\boldsymbol{E}_{\perp}\times\boldsymbol{B}$ drift,

$$\boldsymbol{v}_{j} \equiv \boldsymbol{\Omega}\times\boldsymbol{r}.$$

# §2 Pulsar Emission Models

If copious charges are (somehow) supplied, they realize a force-free magnetosphere, $\boldsymbol{E}\cdot\boldsymbol{B}=0$, and corotate with the magnetosphere under the corotational electric field,

$$\boldsymbol{E}_{\perp} \equiv -c^{-1}(\boldsymbol{\Omega}\times\boldsymbol{r})\times\boldsymbol{B}.$$

Decoupling $\boldsymbol{E}$ into $\boldsymbol{E}_{\perp}$ and $\boldsymbol{E}_{\text{non-corotate}}$, we obtain from the Maxwell eq.

$$\nabla\cdot(\boldsymbol{E}_{\perp}+\boldsymbol{E}_{non-corotate})=4\pi\rho,$$

that is,

$$\nabla\cdot\boldsymbol{E}_{non-corotate}=4\pi(\rho-\rho_{GJ}),$$

where $\rho_{GJ}\equiv \nabla\cdot\boldsymbol{E}_{\perp}\sim -\boldsymbol{\Omega}\cdot\boldsymbol{B}$.

If $\rho$ deviates from $\rho_{GJ}$ in some region,
$E_{\parallel}=\boldsymbol{E}_{non-corotate}\cdot\boldsymbol{B}/B$ arises around that region.

Thus, the problem reduces to …

"Where and how does the charge deficit ($|\rho|<|\rho_{GJ}|$) appear?"

Decoupling $\boldsymbol{E}$ into $\boldsymbol{E}_{\perp}$ and $\boldsymbol{E}_{\text{non-corotate}}$, we obtain from the Maxwell eq.

$$\nabla\cdot(\boldsymbol{E}\downarrow\perp+\boldsymbol{E}\boldsymbol{non-corotate})=4\pi\rho,$$

that is,

$$\nabla\cdot\boldsymbol{E}\boldsymbol{non-corotate}=4\pi(\rho-\rho_{GJ}),$$

where $\rho_{GJ}\equiv\nabla\cdot\boldsymbol{E}\downarrow\perp\sim-\boldsymbol{\Omega}\cdot\boldsymbol{B}.$

If $\rho$ deviates from $\rho_{GJ}$ in some region,
$E_{\parallel}=\boldsymbol{E}\boldsymbol{non-corotate}\cdot\boldsymbol{B}/\mathrm{B}$ arises around that region.

# §2 Pulsar Emission Models

Early 80's, the polar-cap (PC) model was proposed.

(Daugherty & Harding ApJ 252, 337, 1982)

A single PC beam can produce a variety of pulse profiles.

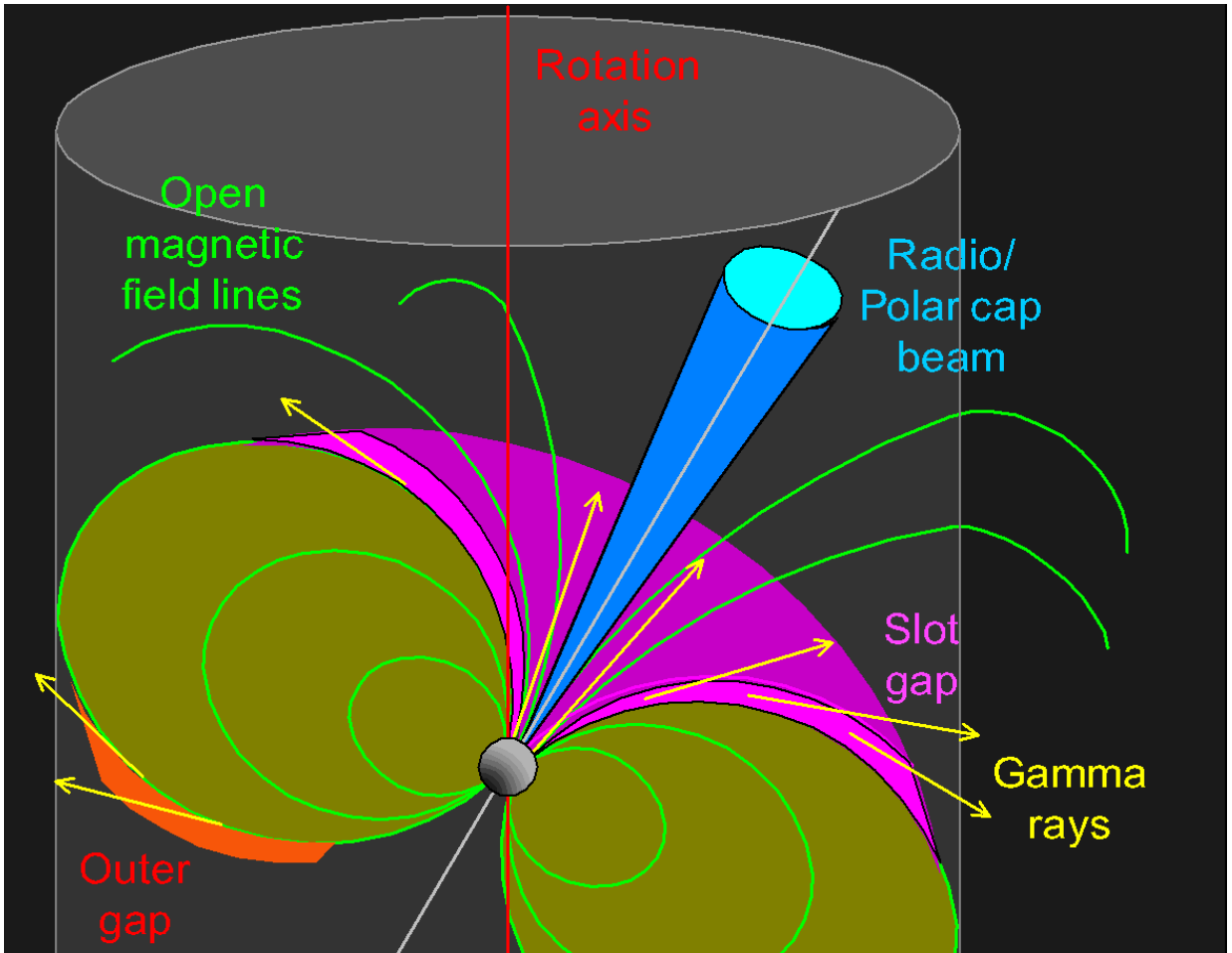

# §2 Pulsar Emission Models

Early 80's, the polar-cap (PC) model was proposed.
(Daugherty & Harding ApJ 252, 337, 1982)

A single PC beam can produce a variety of pulse profiles.

However, the emission solid angle ($\Delta\Omega$ «1 ster) was too small to reproduce the wide-separated double peaks.

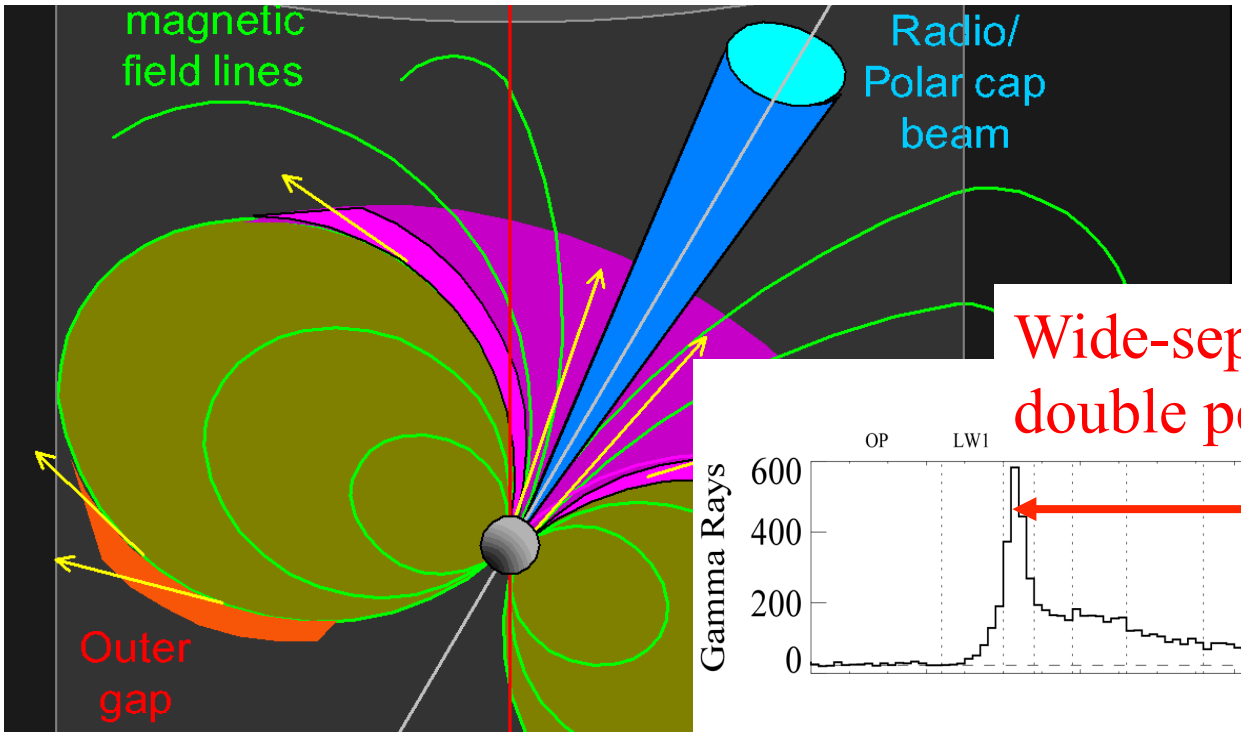

# §2 Pulsar Emission Models

Early 80's, the polar-cap (PC) model was proposed.
(Daugherty & Harding ApJ 252, 337, 1982)

A single PC beam can produce a variety of pulse profiles.

However, the emission solid angle ($\Delta\Omega$ «1 ster) was too small to reproduce the wide-separated double peaks.

In addition, localization of gap altitudes («$r_*$) lead to too small $L_\gamma$ («$0.3L_{spin}$), although $L_{radio}\sim10^{-5}L_{spin}$ is OK.

Moreover, the detection of VHE (>20GeV) pulsed emission from the Crab pulsar, which should avoid strong magnetic absorption, clearly rules out PC emissions.

Thus, a high-altitude emission drew attention.

# §2 Pulsar Emission Models

Higher-altitude emission models concentrate on …

- **slot-gap (SG) model** (Muslimov & Harding 2003, 2004)
- **pair- starved polar-cap (PSPC) model** (Venter + 2009)
- **outer gap (OG) model** (Cheng + 1986; Romani 1996)
- **striped-wind synchrotron (SWS) model** (Petri 2013)
- **wind-inverse-Compton (WIC) model** (Aharonian + 2012)

SG, PSPC models: $e^-$ are extracted as in PC model

OG model: $e^{\pm}$'s created by γ-γ coll. and accelerated by $E_{\parallel}$

SWS model: HE pulsed photons emitted from current sheet

WIC model: VHE pulsed photons emitted via ICS by ultra-relativistic $e^{\pm}$'s accelerated at $r < 50\ R_{LC}$

# §2 Pulsar Emission Models

SG model, classic OG models:

have very thin meridional thickness ($w \ll 1$),

reproduce only $10^{-1}$~$10^{-3}$ $L_\gamma$ (KH 2008 ApJ 688, L25)

Therefore, the PSPC model ($w \leq 1.0$) was proposed.

However, the PSPC model contradicts with $div(\boldsymbol{B})=4\pi\rho$, in the same way as the SG model.

(KH 2011, High Energy Emission from Pulsars and Their Systems, p. 117–37)

Thus, as long as the emissions **inside LC** are concerned, the modern OG model ($w>0.1$), survives as the only model that quantitatively describes the pulsed HE/VHE emissions.

However, in all the models above, ***B*** configuration is <u>not</u> solved consistently with the magnetospheric currents.

# §2 *Pulsar Emission Models*

How about the emissions **outside the light cylinder**?

To set up the SWS or WIC model, we must introduce different physical mechanisms from SG/PSPC/OG models.

In the SWS model, plasma collective effects (e.g., wave-particle interactions) are considered as a heating mechanism of plasmas in the current sheet. Chkheidze + (2013)
Although, ***B*** configuration is consistently solved, particle creation & acceleration are artificially set up.

Bai & Spitkovski (ApJ, 715, 1270; 1282, 2010a,b)

In the WIC model, the physical mechanism that converts the Poynting energy into the plasmas' kinetic energy has not been solved. Aharonian + (Nature, 482, 507, 2012 )

# §2 Pulsar Emission Models

The ***B*** structure can be solved e.g., by the **PIC simulation**.

This approach is valid for **coherent pulsar radio** emissions.

(1) A bunch of electrons move in phase in PC region.

Plasma collective effects essential for coherent emi.
PIC solves from first principles. (Timokhin, Arons 2013)

(2) Spatial size < coherent scale (<50 cm at 600 MHz)

The microscopic cell size in the PIC code favors such localized phenomena (e.g., strong shocks)

However, such exact treatment are unnecessary to study **incoherent high-energy** (> 0.001 eV) emissions, because

(1) plasma collective effects are negligible as $\nu > \nu_{plasma}$,

(2) spatial size >1000 km for typical young pulsars.

Microscopic PIC cell size disfavors such non-localized phenomena.

# §2 Pulsar Emission Models

It is, therefore, possible to investigate incoherent pulsar HE/VHE emissions by solving the set of

(1) $e^{\pm}$ Boltzmann equations,

(2) radiative transfer equation, and

(3) the Poisson equation for the electro-static potential

(i.e., $\nabla \cdot \mathbf{E} = 4\pi\rho$),

without taking account of plasma collective effects in the Boltzmann equations.

Instead of solving the ***B*** field configuration near the light cylinder, we parameterize how the vacuum dipole ***B*** field is deformed into monopole-like, and compare the prediction with the γ-ray observations.

# §2 Pulsar Emission Models

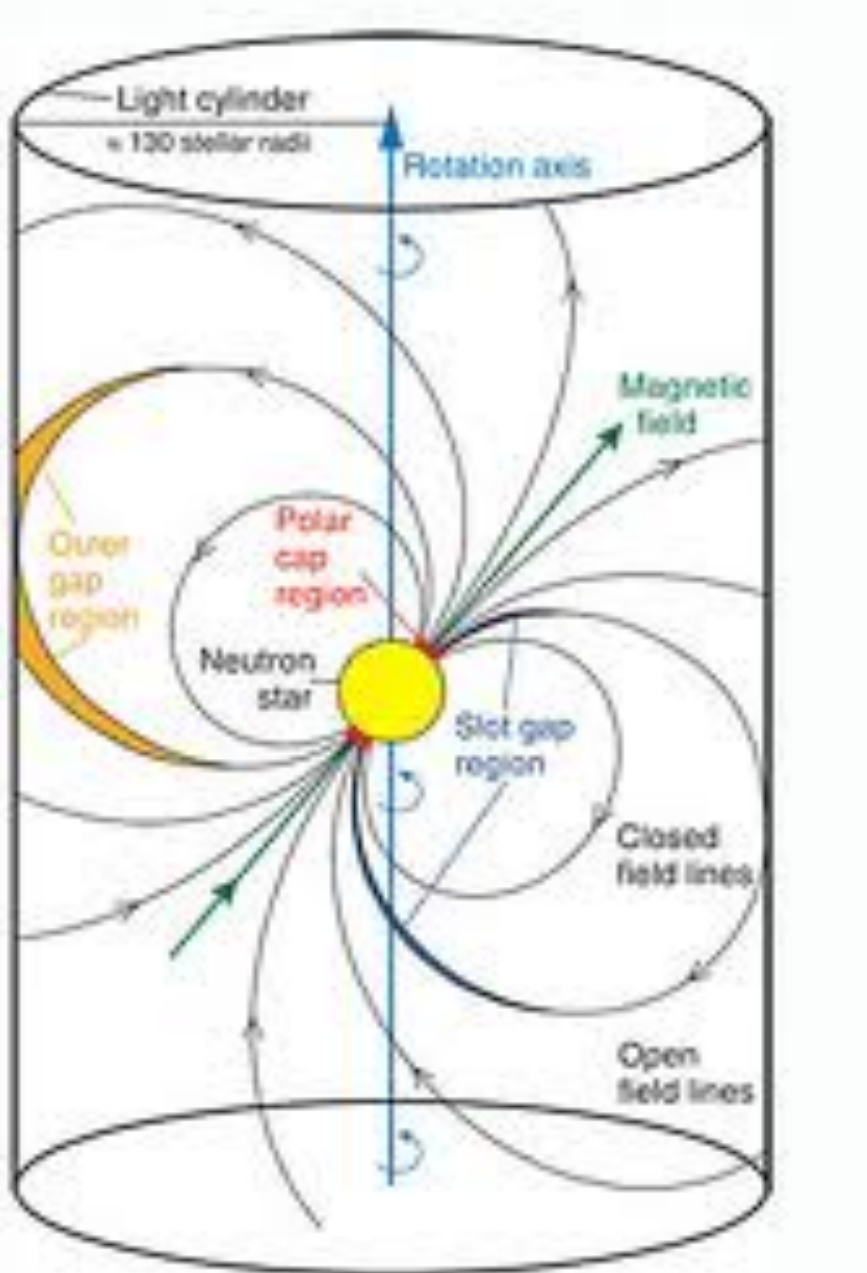


As a model of high-altitude emissions, we investigate the outer gap scenario.

Cheng, Ho, Ruderman (1986, ApJ 300, 500)

Emission altitude

~ light cylinder

⟶ hollow cone emission ($\Delta\Omega > 1$ ster)

OG model was further developed by including special relativistic effects.

Romani (1996, ApJ 470, 469)

# §2 Pulsar Emission Models

Successfully explained wide-separated double peaks

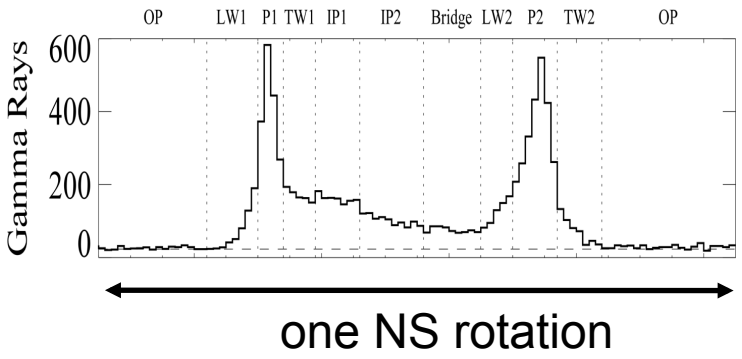


OG model became promising.

As an alternative possibility of high-altitude emission model, the outer gap model was proposed.

Cheng, Ho, Ruderman (1986, ApJ 300, 500)

Emission altitude > 100 $r_{NS}$
⟶ hollow cone emission
($\Delta\Omega > 1$ ster)

OG model was further developed by including special relativistic effects.

Romani (1996, ApJ 470, 469)

# §2 Pulsar Emission Models

Indeed, the VHE pulsed emission (>100MeV) from the Crab pulsar shows that these γ-rays are emitted from the **outer** magnetosphere (~~$\gamma B \rightarrow ee$~~).

We thus consider the outer-gap model (Cheng+ 86, ApJ 300,500) in this talk.

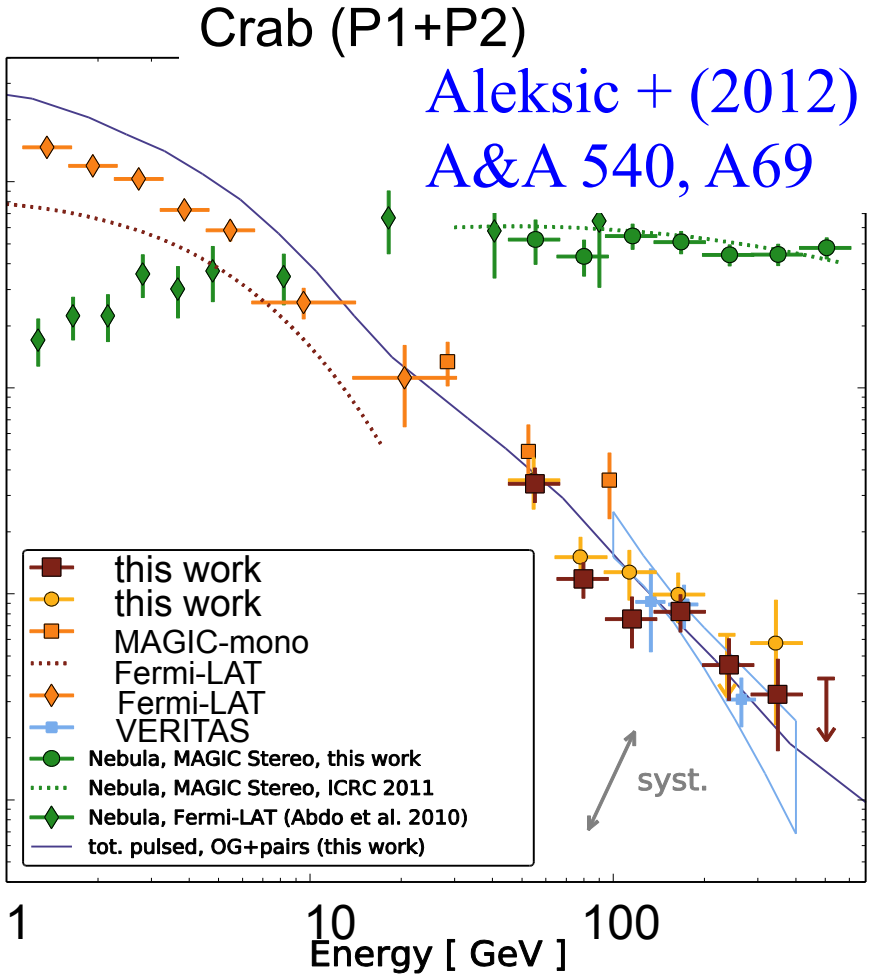

# §2 Pulsar Emission Models

Various attempts have been made on recent OG model:

3-D geometrical model

→ phase-resolved spectra (Cheng + '00; Tang + '08)

→ atlas of light curves for PC, OG, SG models (Watters + '08)

2-D self-consistent solution (Takata + '06; KH '06)

3-D self-consistent solution

→ phase-resolved spectra, absolute luminosity if we give only $P$, $dP/dt$, $\alpha$, $kT$ ($+\zeta$) (this talk)

In this talk, I'll present the most recent results obtained in my 3-D version of self-consistent OG calculations.

# §3 Modern Outer-gap Model: Formalism

I quantify the classic OG model by simultaneously solving the pair-production cascade in a rotating NS magnetosphere:

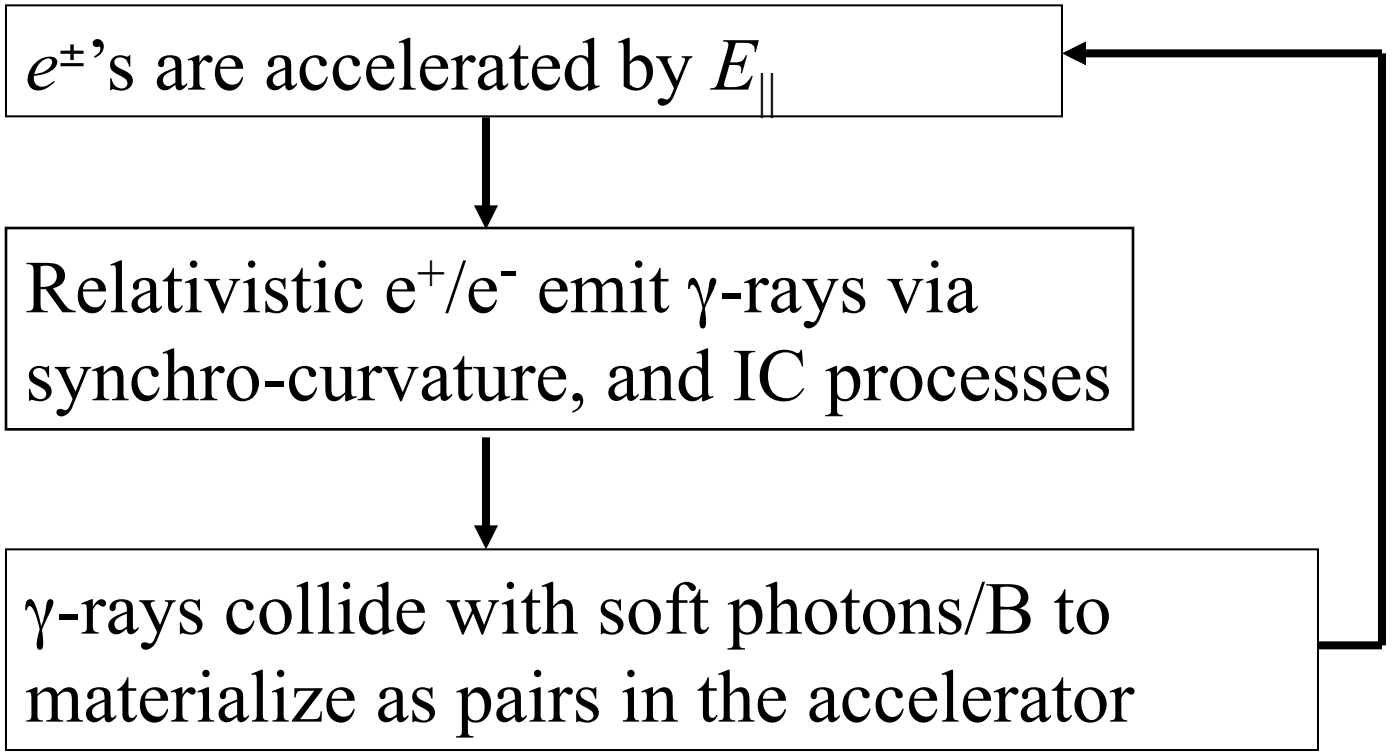

# §3 Modern OG Model: Formalism

Poisson equation for electrostatic potential $\psi$ :

$$-\nabla^2\psi = -\frac{\partial^2\psi}{\partial x^2} - \frac{\partial^2\psi}{\partial y^2} - \frac{\partial^2\psi}{\partial z^2} = 4\pi(\rho - \rho_{\rm GJ}) \ ,$$

where

$$E_{\parallel} = -\frac{\partial\Psi}{\partial x}, \ \rho_{\rm GJ} = \frac{\mathbf{\Omega}\cdot\mathbf{B}}{2\pi c} \ ,$$

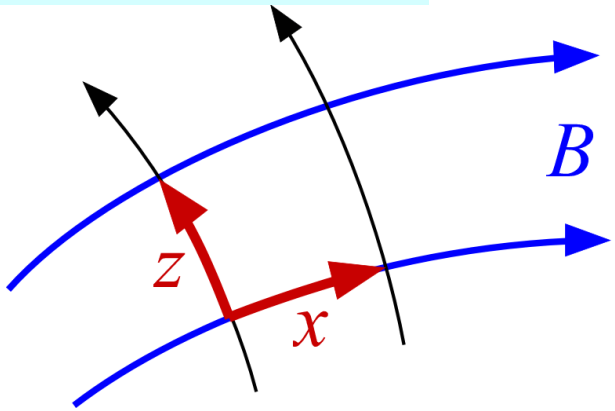


$$\rho(\mathbf{x}) \equiv e\int_1^{\infty} d\gamma \int_0^{\pi} d\chi \left[N_+(\mathbf{x},\gamma,\chi) - N_-(\mathbf{x},\gamma,\chi)\right] + \rho_{\rm ion}(\mathbf{x}),$$

$\mathbf{x} = (x, y, z)$ .

$N_+/N_-$: distrib. func. of $e^+/e^-$

$\gamma$ : Lorentz factor of $e^+/e^-$

$\chi$ : pitch angle of $e^+/e^-$

# §3 Modern OG Model: Formalism

Assuming $\partial_t+\Omega\partial_\phi=0$ , we solve the $e^{\pm}$'s Boltzmann eqs.

$$\frac{\partial N_{\pm}}{\partial t}+\mathbf{v}\cdot\nabla N_{\pm}+\left(e\mathbf{E}_{\|}+\frac{\mathbf{v}\times\mathbf{B}}{c}\right)\cdot\frac{\partial N_{\pm}}{\partial \mathbf{p}}=S_{IC}+S_{SC}+\int\alpha_\nu d\nu\int\frac{I_\nu}{h\nu}d\omega$$

together with the radiative transfer equation,

$$\frac{dI_\nu}{dl}=-\alpha_\nu I_\nu+j_\nu$$

$N_{\pm}$: positronic/electronic spatial # density,
$E_{\|}$: mangnetic-field-aligned electric field,
$S_{\rm IC}$: ICS re-distribution function, $d\omega$: solid angle element,
$I_\nu$: specific intensity, $l$ : path length along the ray
$\alpha_\nu$: absorption coefficient, $j_\nu$: emission coefficient

# §3 Modern outer-gap model

Application to a typical young pulsar ($\tau$=*3* kyr),

$P$=*54* ms, $\mu$=3.2×10$^{30}$ G cm$^3$, $\alpha$=60$^o$ , $kT$= 60 eV

Recent force-free, MHD, and PIC simulations suggest that ***B*** field approaches **monopole-like** near and beyond the light cylinder.

However, for simplicity, we consider a current-free, rotating dipole ***B*** today.

Maxwell & Boltzmann eqs., ⇒

- OG 3-D geometry,
- $E_{\parallel}$ distribution,
- $e^+/e^-$ distribution functions,
- photon specific intensity

# §3 Outer-gap model

3-D distribution of the particle accelerator (i.e., high-energy emission zone) solved from the Poisson eq.:

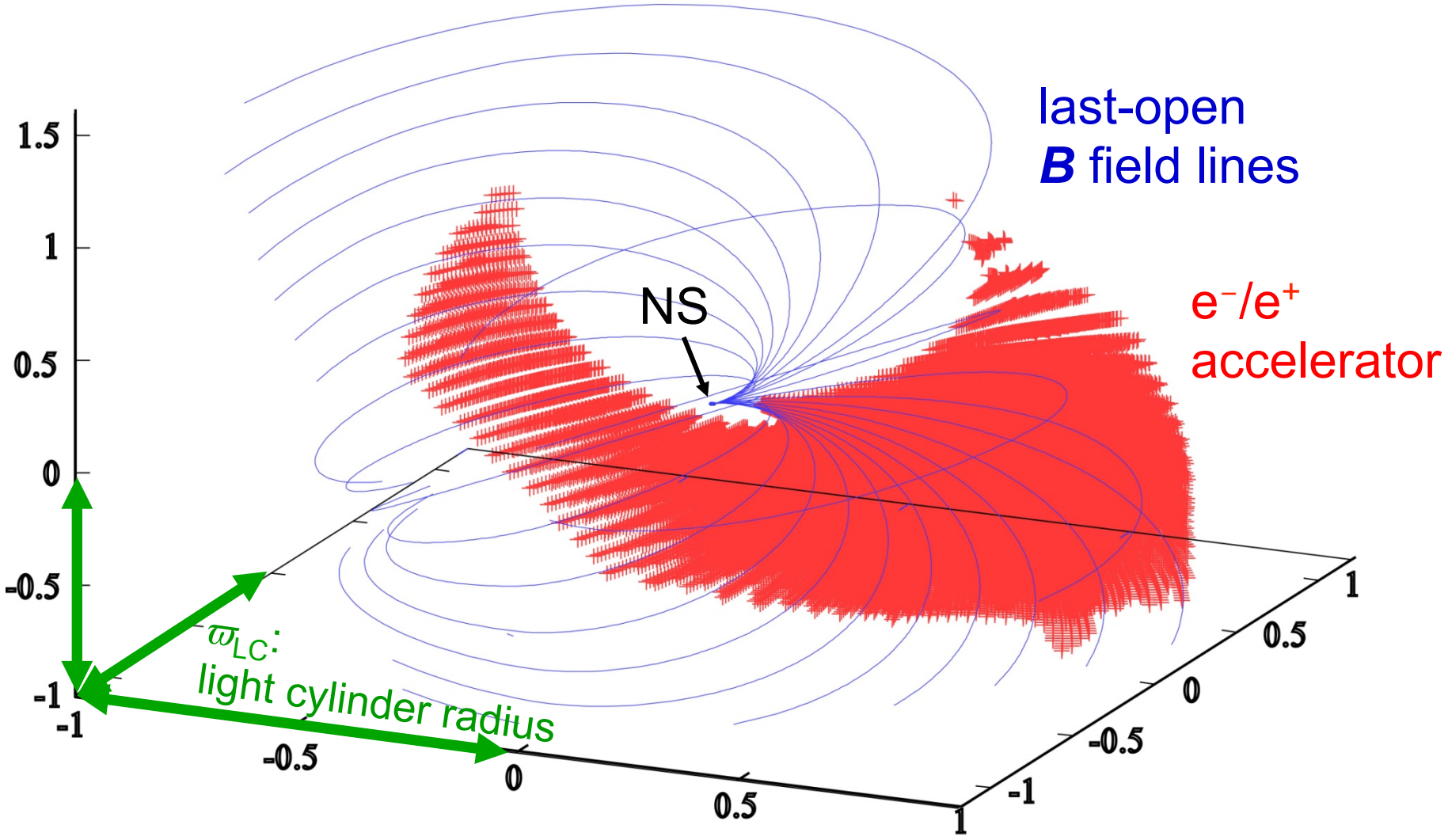

# §3 Outer-gap model

3-D distribution of the particle accelerator (i.e., high-energy emission zone) solved from the Poisson eq.:

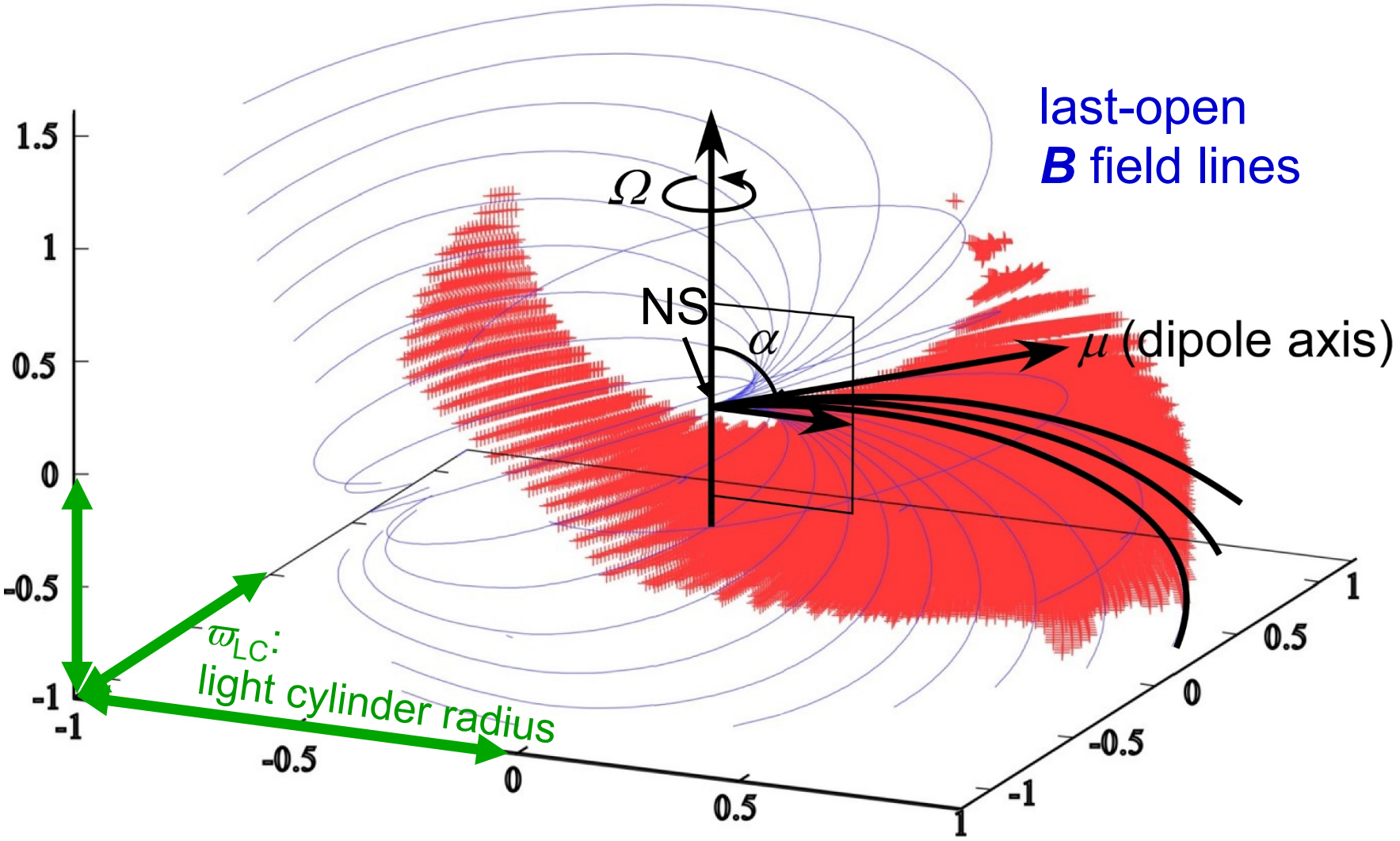

# §3 Vacuum, classic 2-D outer-gap model

***B***-field-aligned ***E*** field (acceleration field) on $\Omega$ -$\mu$ plane:

$E_{||}$ maximizes along meidionally middle-height ***B*** lines.

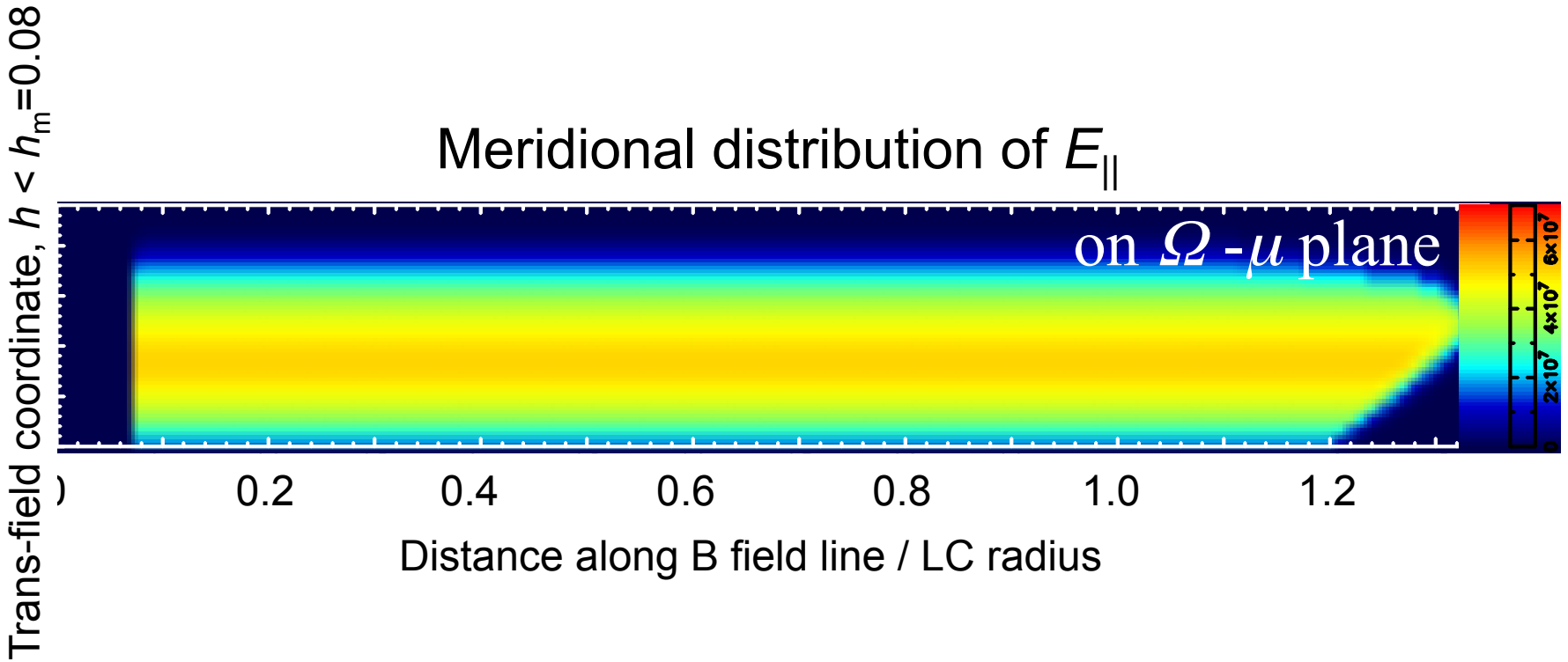


Vacuum 2-D outer-gap solution

# §3 Vacuum, classic 2-D outer-gap model

To consider emission from a 3-D magnetosphere, assume that the same $E_{||}$ extends in azimuthal direction.

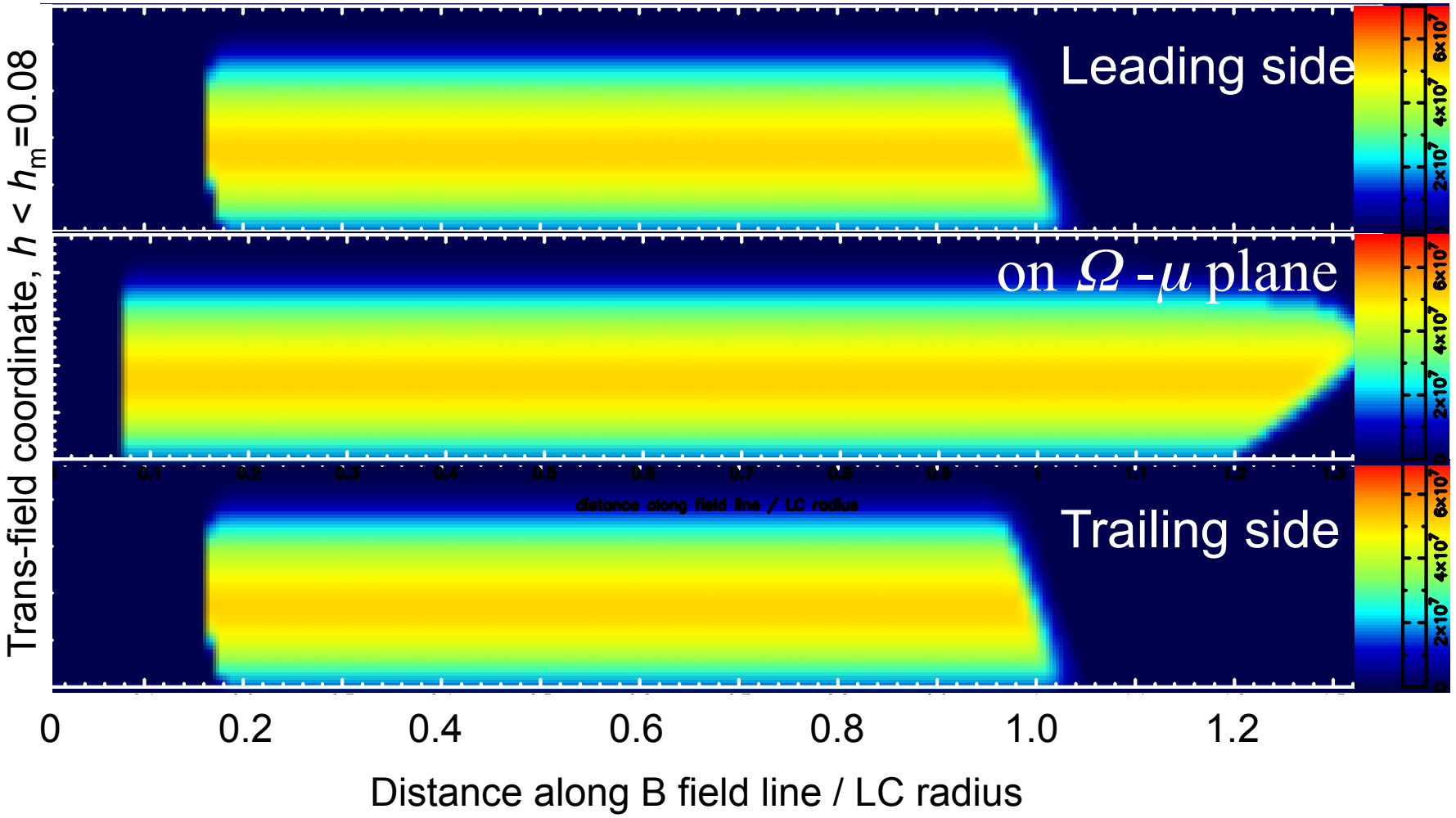

# §3 Vacuum, classic 2-D outer-gap model

The maximum $E_{||}$ (in the meridional direction) is projected on the last-open ***B*** field surface.

$E_{||}$ for vacuum, rotating dipole ***B*** field ($b$=0 case)

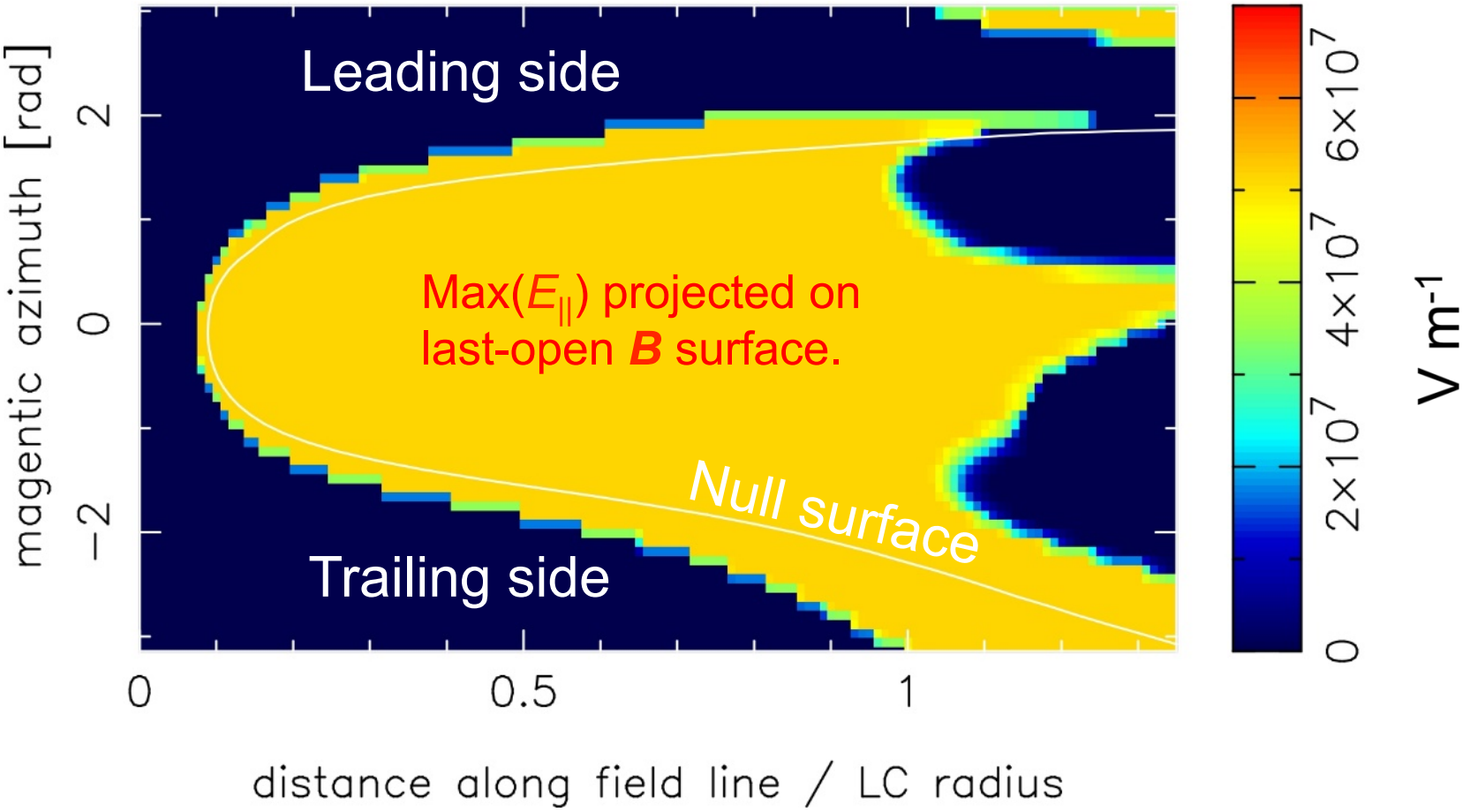

# §3 Vacuum, classic 2-D outer-gap model

The maximum $E_{||}$ (in the trans-field direction) is projected on the last-open ***B*** field surface.

$E_{||}$ for vacuum, rotating dipole ***B*** field ($b$=0 case)

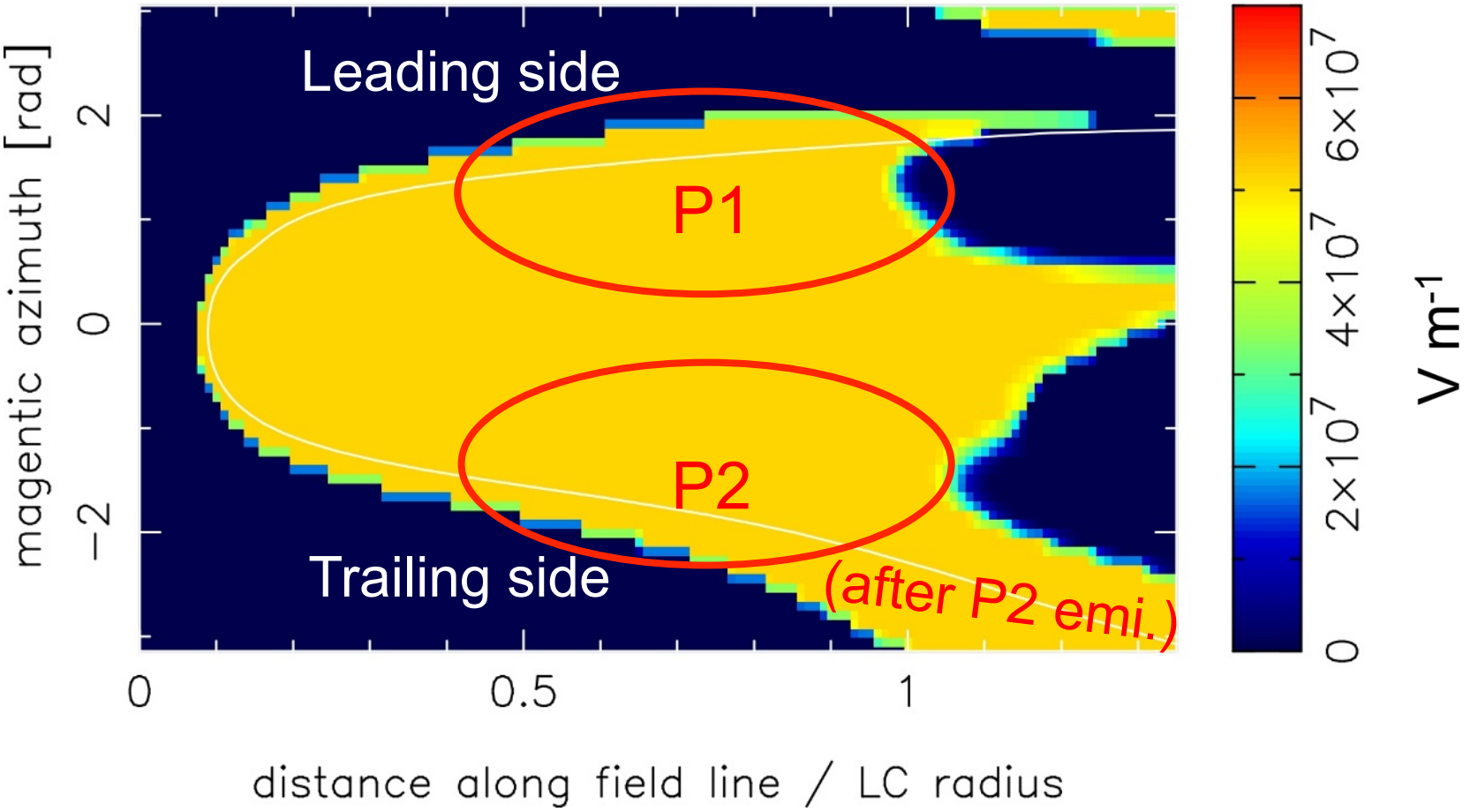

# §3 Vacuum, classic 2-D outer-gap model

Pulse profile at four different observer's viewing angles.

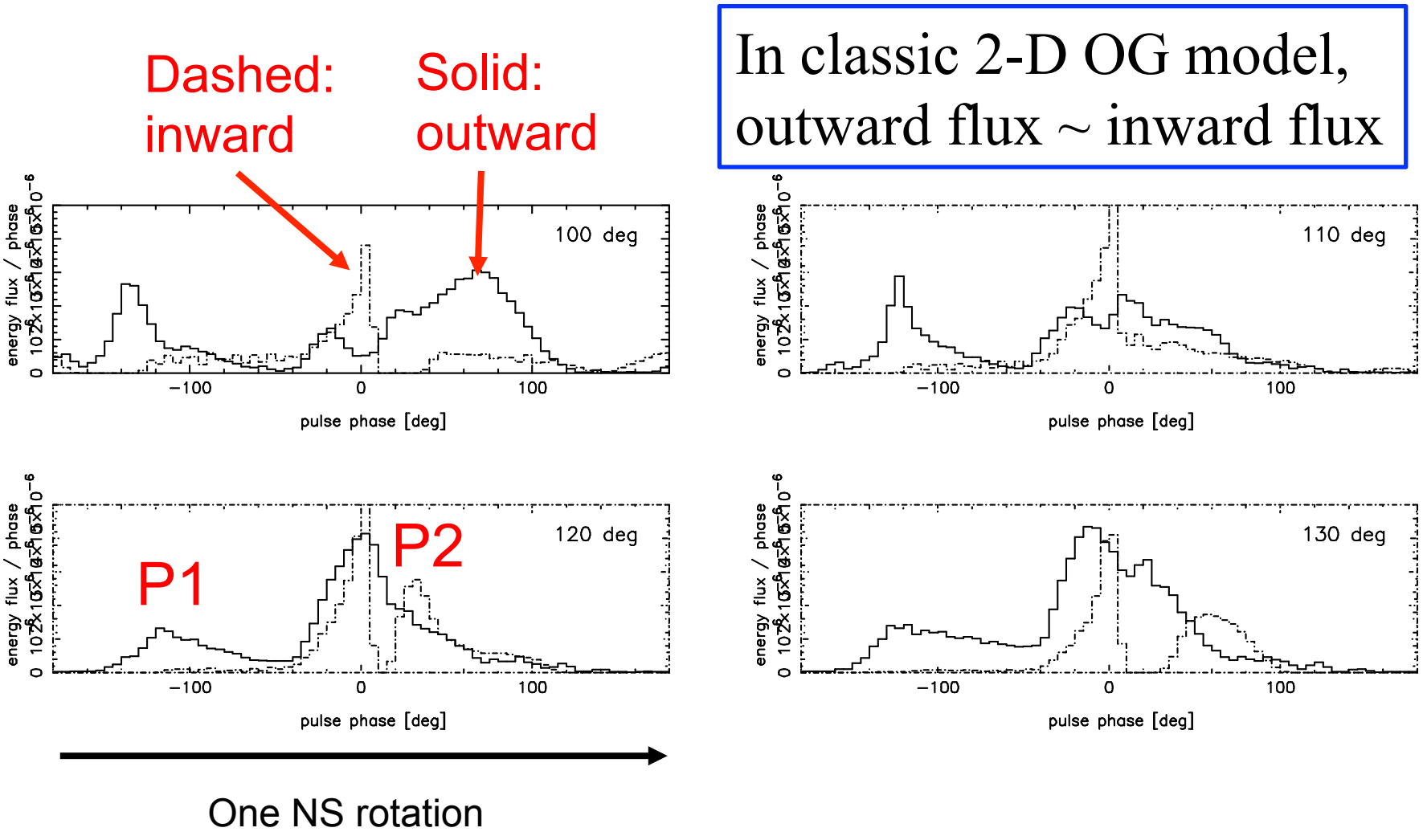

# §3 Outer-gap model

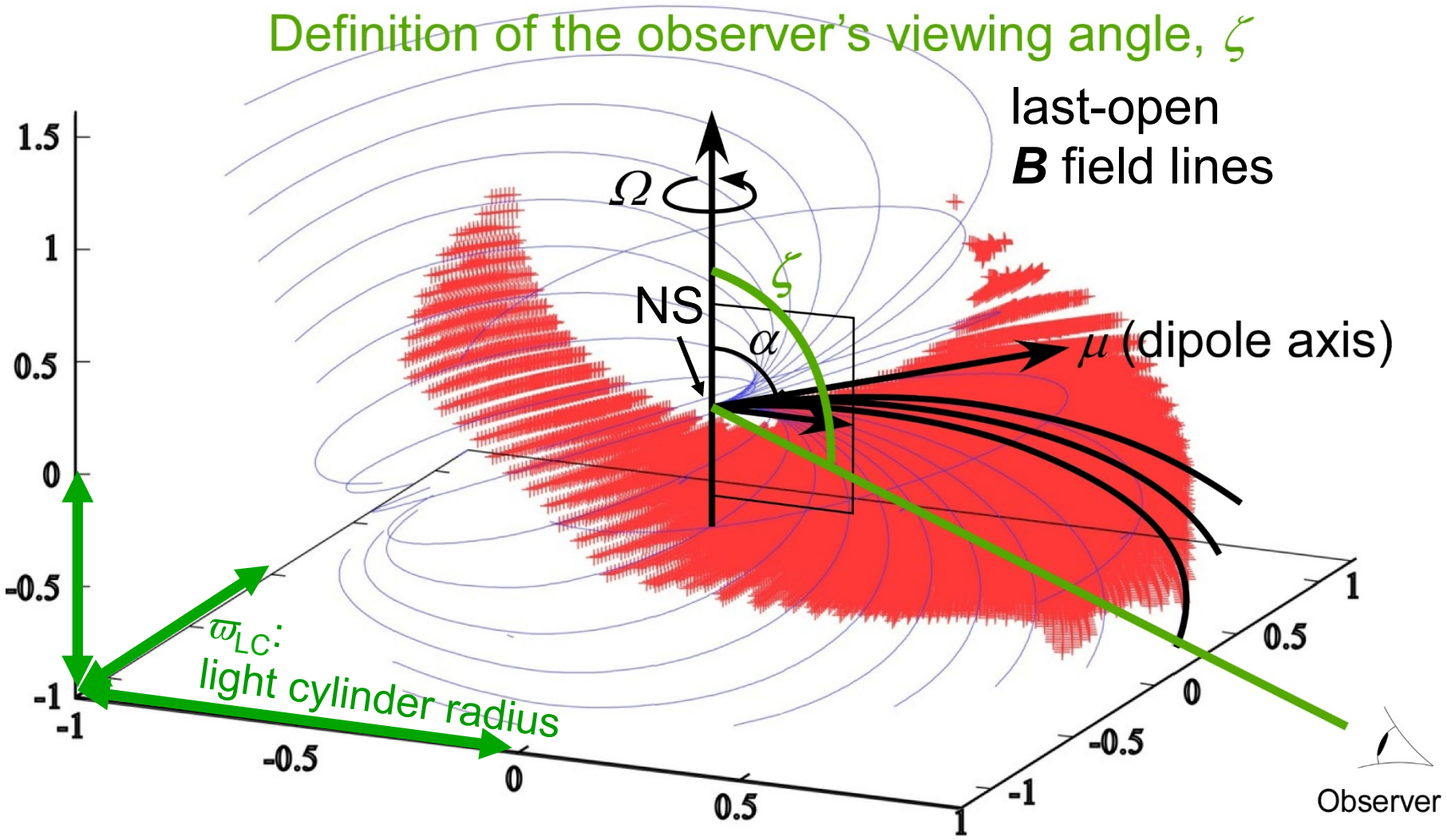

# §3 Vacuum, classic 2-D outer-gap model

Pulse profile at four different observer's viewing angles.

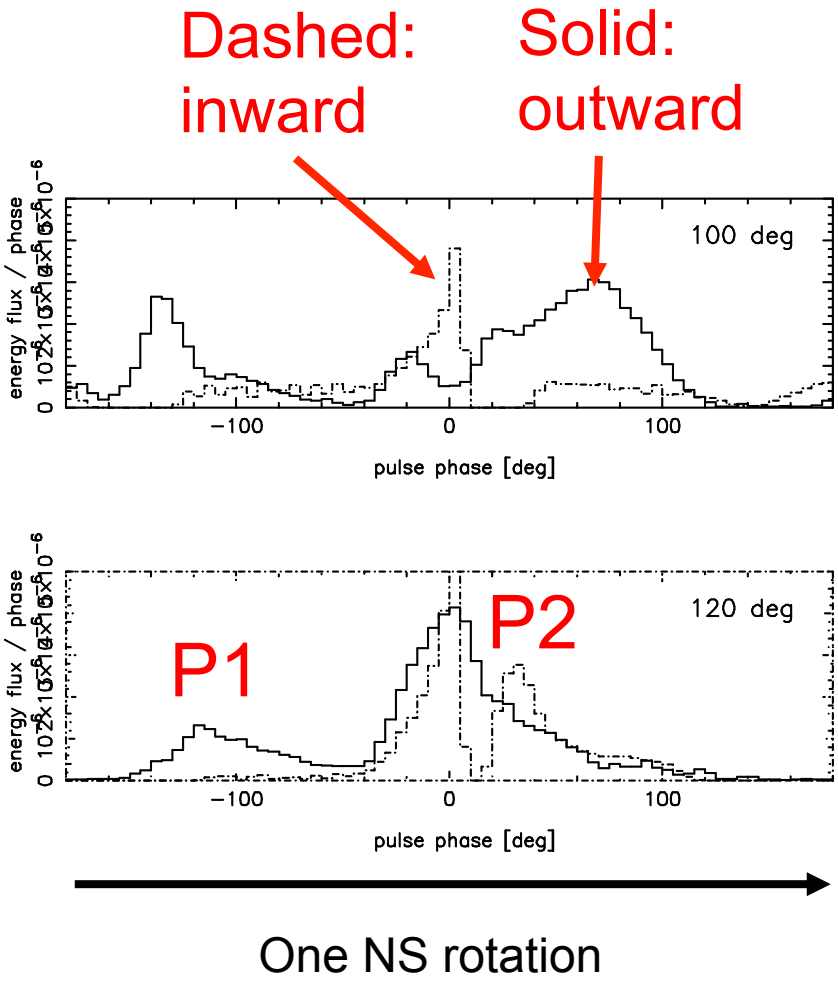


In classic 2-D OG model, outward flux ~ inward flux

At $80^o<\zeta<100^o$, it results in more than two peaks, which contradicts w/ γ-ray observations.

Thus, in all previous OG models, inward « outward has been assumed.

# §3 Vacuum, classic 3-D outer-gap model

We next solve the Poisson eq. in 3-D pulsar magnetosphere, under $\rho=0$.

$E_{||}$ distribution on the meridional plane:

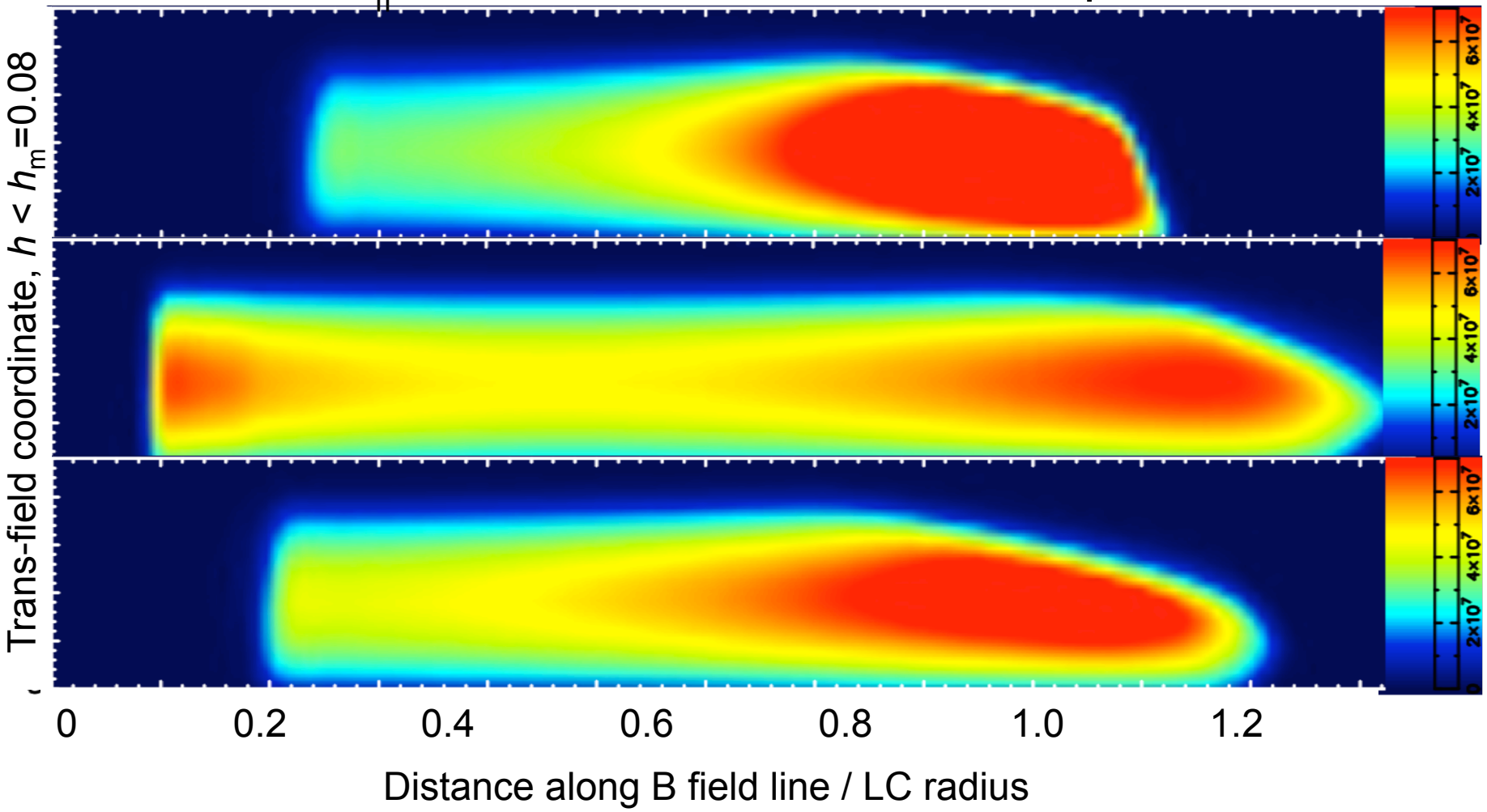

# §3 Vacuum, classic 3-D outer-gap model

Stronger $E_{\parallel}$ appears near the light cylinder.

$E_{\parallel}$ projected on the last-open B field surface:

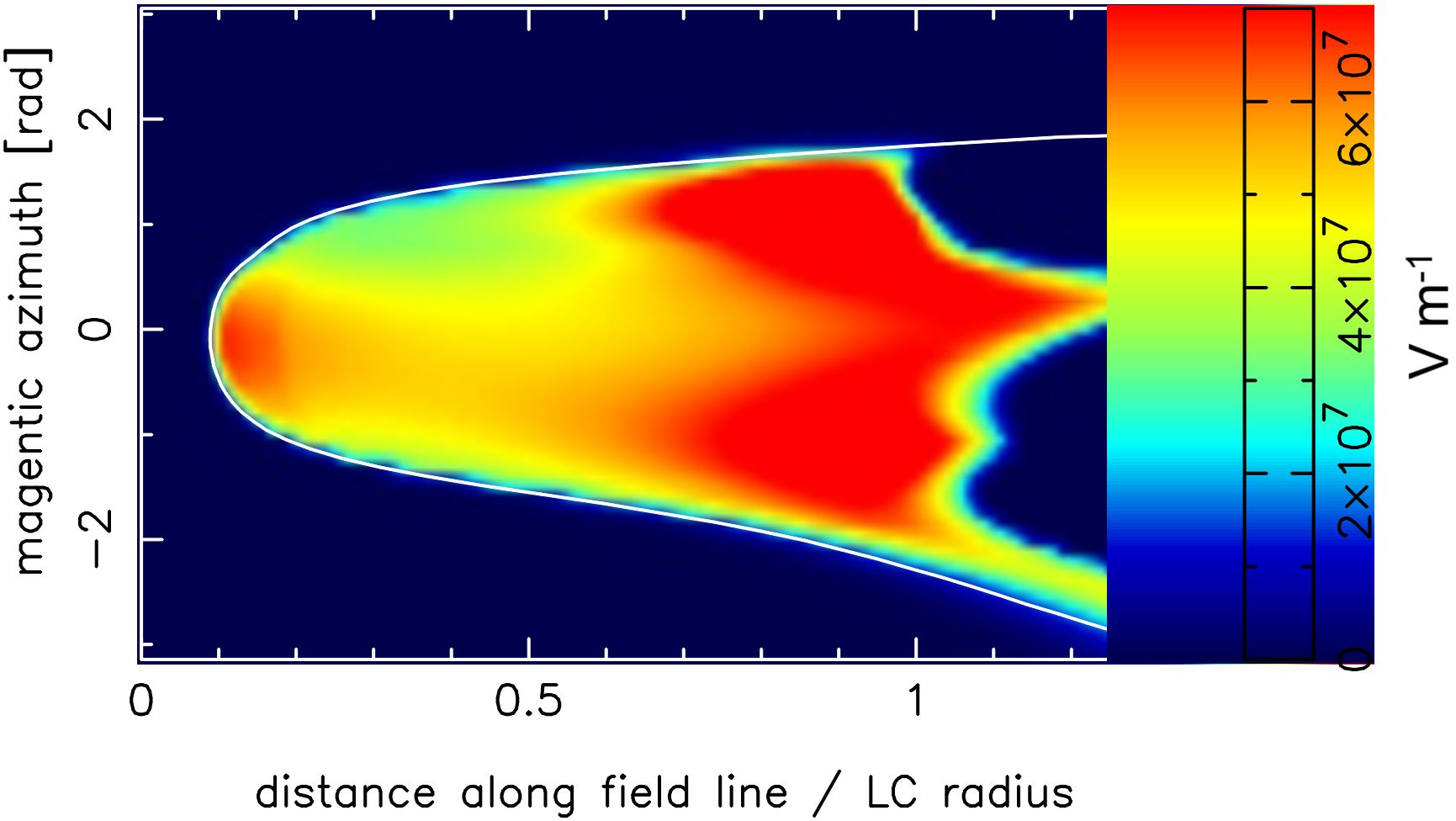

# §3 Vacuum, classic 3-D outer-gap model

Vacuum $E_{||}$ is determined by the $\rho_{GJ}$ gradient, which is solely determined by $\boldsymbol{B}$ geometry.

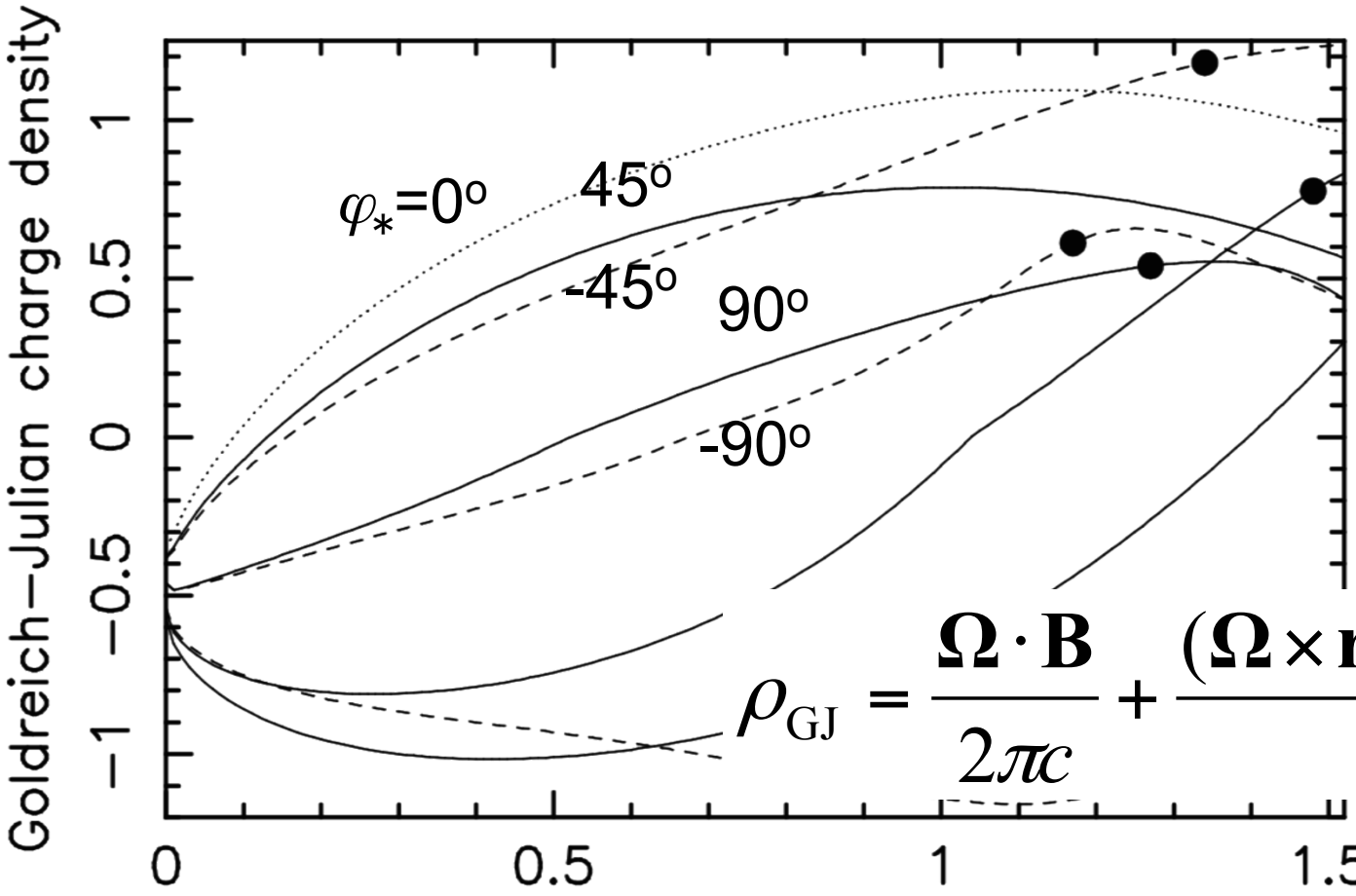


Pure dipole $b$=0.

$$\rho_{GJ} = \frac{\boldsymbol{\Omega}\cdot\mathbf{B}}{2\pi c} + \frac{(\boldsymbol{\Omega}\times\mathbf{r})\cdot(\nabla\times\mathbf{B})}{4\pi c}$$

KH 2014, MNRAS 442, L43

# §3 Vacuum, classic 3-D outer-gap model

Vacuum $E_{||}$ is determined by the $\rho_{GJ}$ gradient, which is solely determined by $\boldsymbol{B}$ geometry.

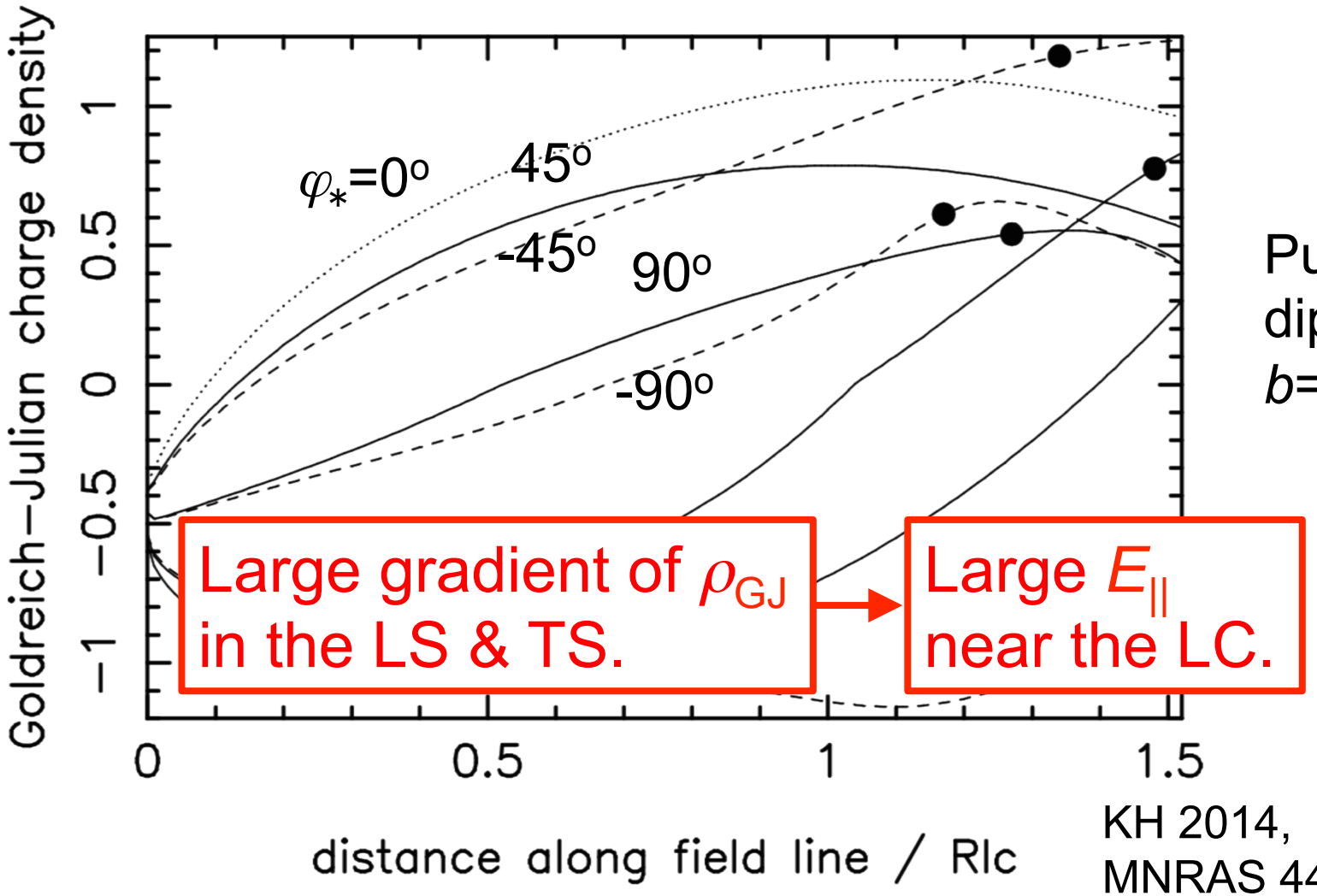


Pure dipole $b$=0.

KH 2014, MNRAS 442, L43

# §3 Vacuum, classic 3-D outer-gap model

Stronger $E_{\parallel}$ appears near the light cylinder.

$E_{\parallel}$ projected on the last-open B field surface:

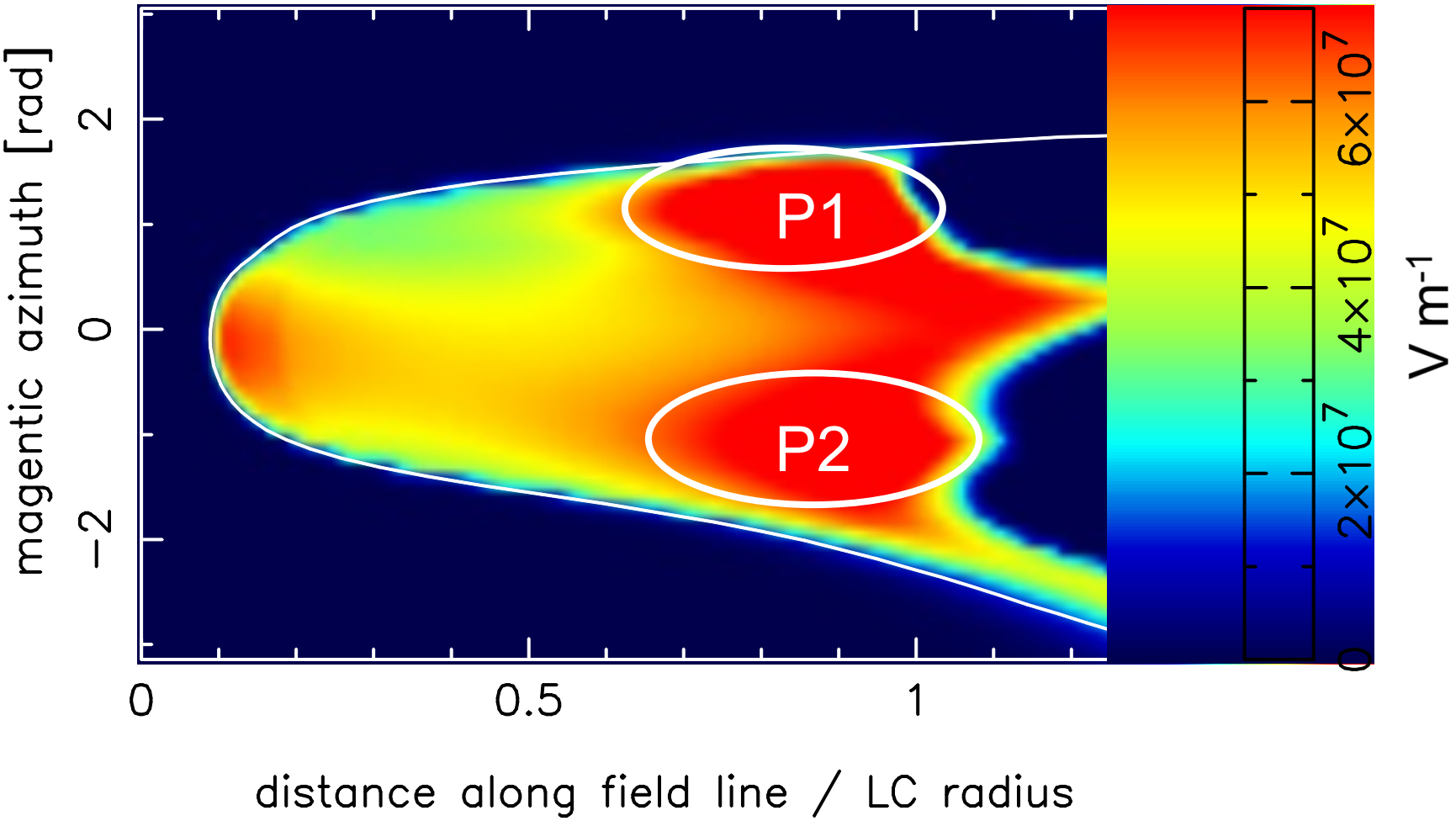

# §3 Vacuum, classic 3-D outer-gap model

Pulse profile at four different observer's viewing angles.

Dashed: inward

Solid: outward

In vacuum 3-D OG model, outward flux ~ inward flux

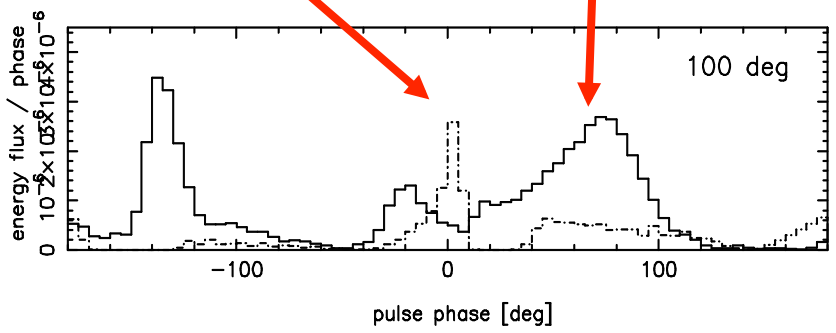


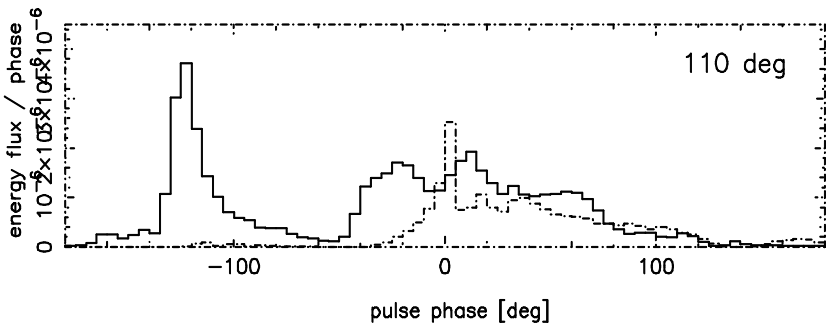


P1

P2

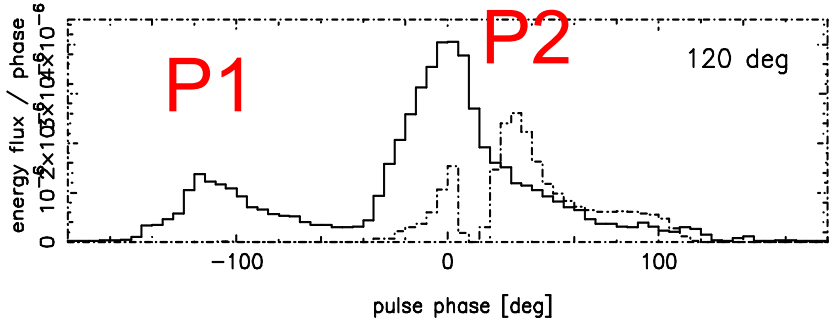


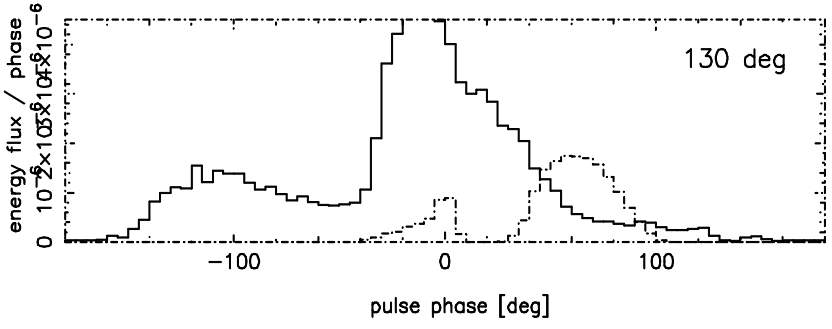


One NS rotation

# §3 Vacuum, classic 3-D outer-gap model

Pulse profile at four different observer's viewing angles.

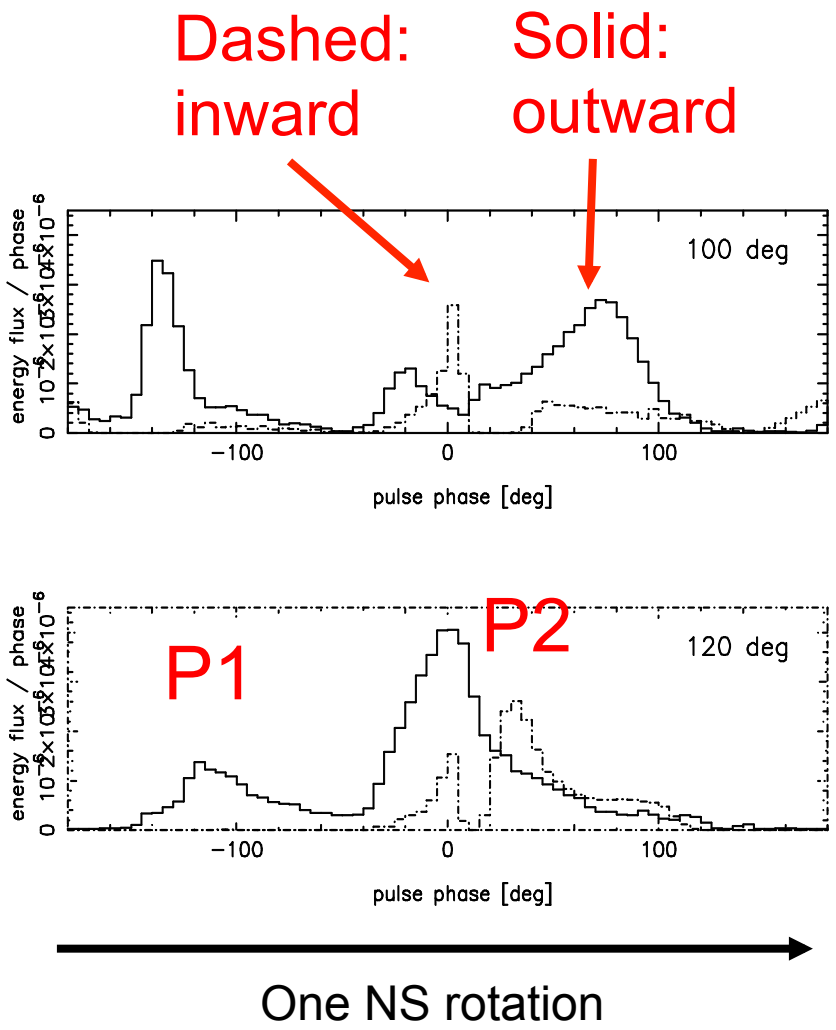


In vacuum 3-D OG model, outward flux ~ inward flux.

We still have more than two peaks at $80^o<\zeta<100^o$.

Thus, we must contrive a model that predicts inward flux « outward flux.

# §3 *Non-vacuum 3-D outer-gap model*

Indeed, we can naturally derive inward flux « outward flux if we consider the screening of $E_{||}$ by solving
(1) The Poisson eq. for electrostatic potential,
(2) Electron/positron Boltzmann eqs., and
(3) Radiative transfer eq.
simultaneously.

KH ApJ 798, L40 (2015)

# §3 Application to the Crab pulsar

We solve the non-vacuum Poisson eq. in 3-D pulsar magnetosphere, under $\rho \neq 0$.

$$-\nabla^2 \Psi = 4\pi(\rho - \rho_{GJ})$$

$E_{||}$ distribution on the meridional plane:

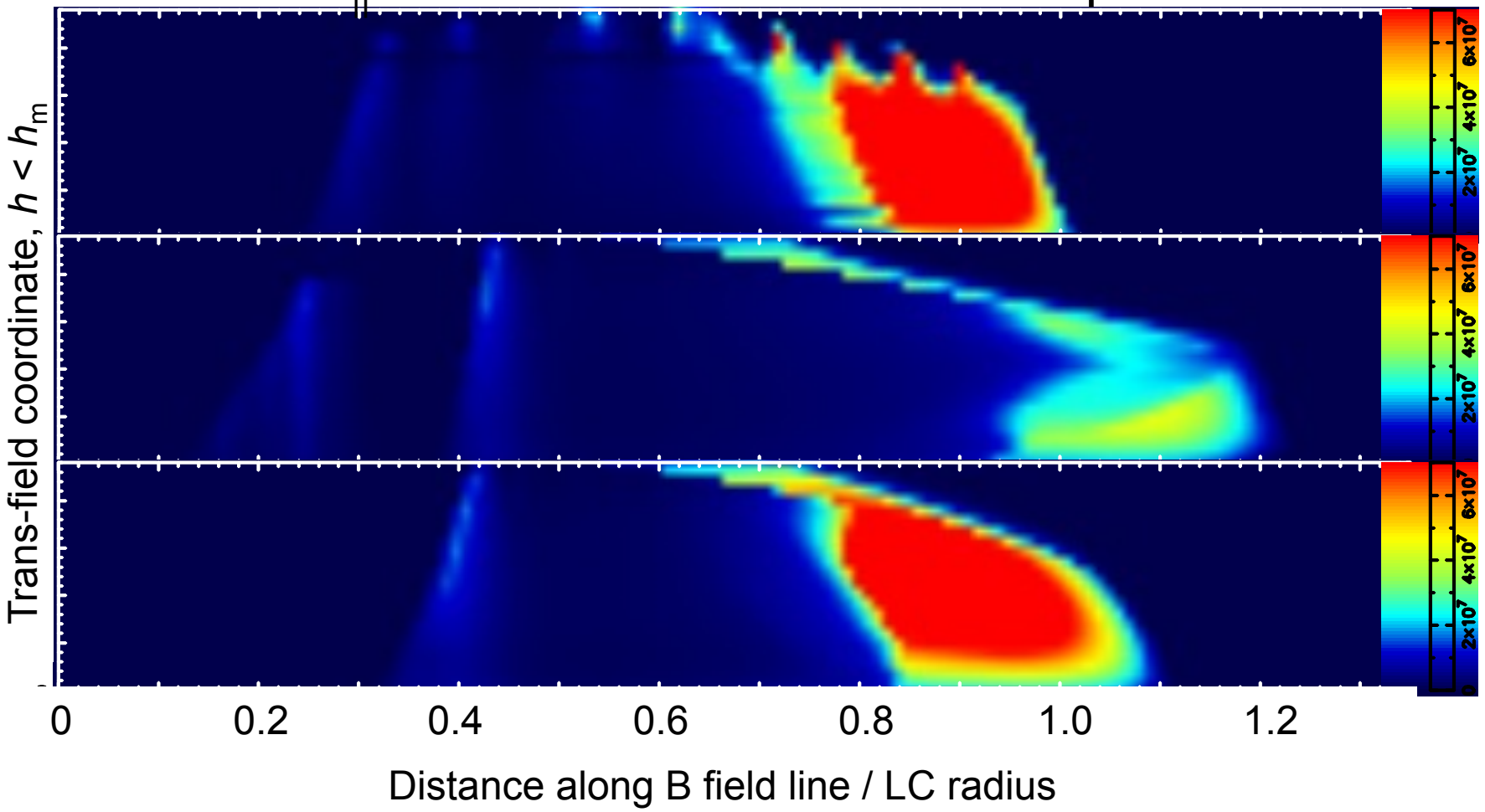

# §3 Application to the Crab pulsar

Stronger $E_{\parallel}$ appears near the light cylinder.

$\max(E_{\parallel})$ projected on the last-open B field surface:

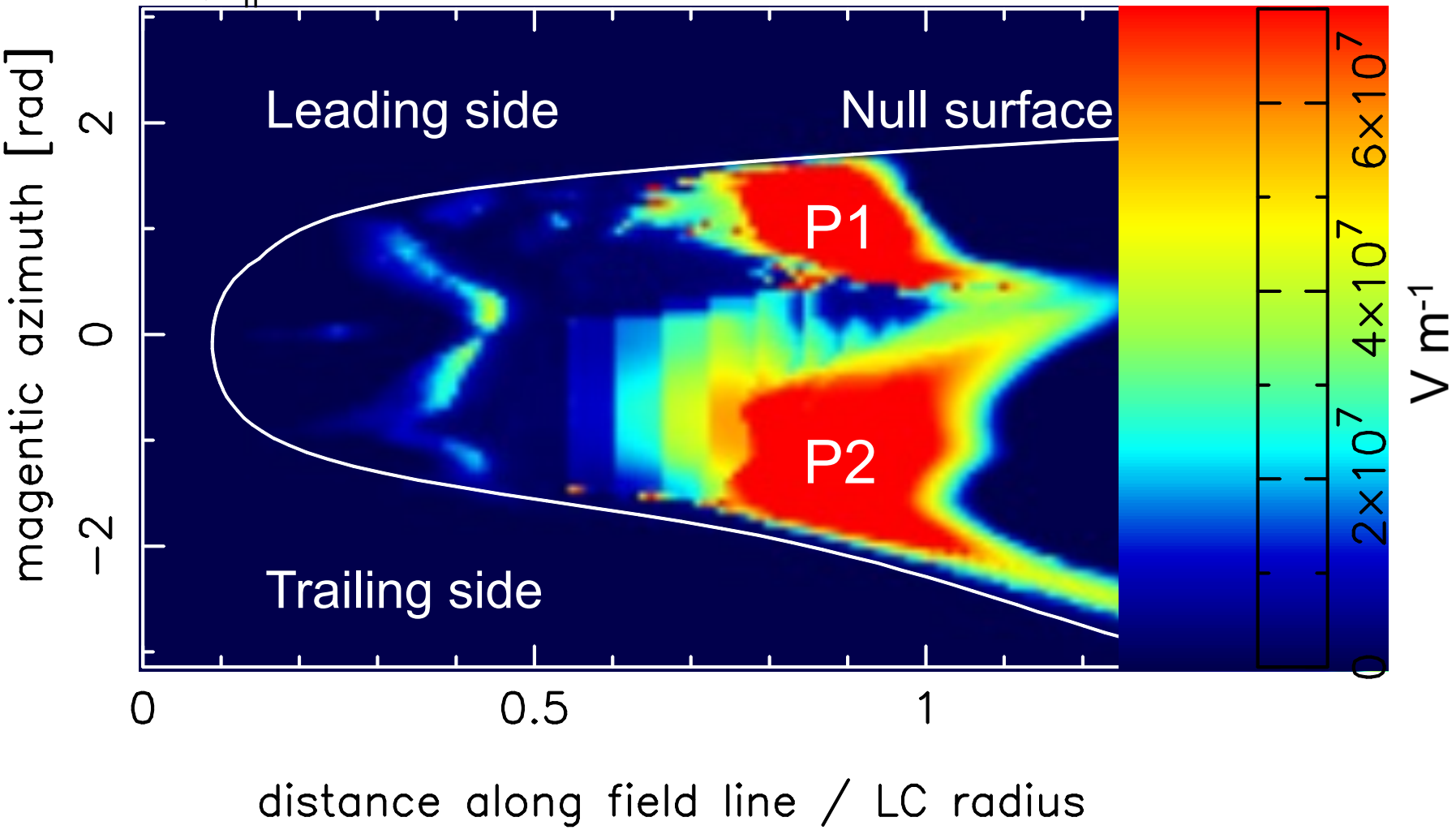

# §3 Non-vacuum 3-D outer-gap model

Pulse profile at four different observer's viewing angles.

In non-vacuum 3-D OG model, outward flux « inward flux.

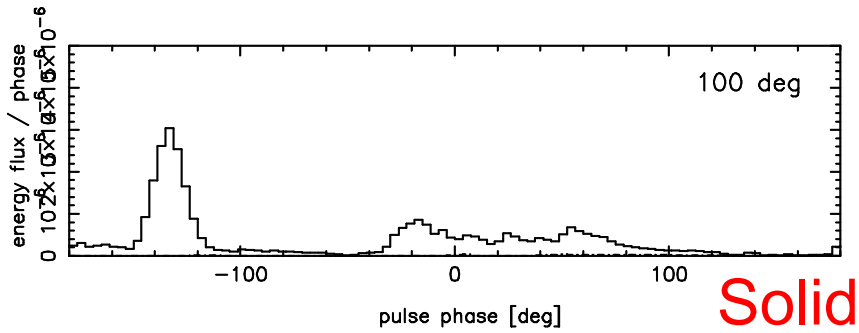


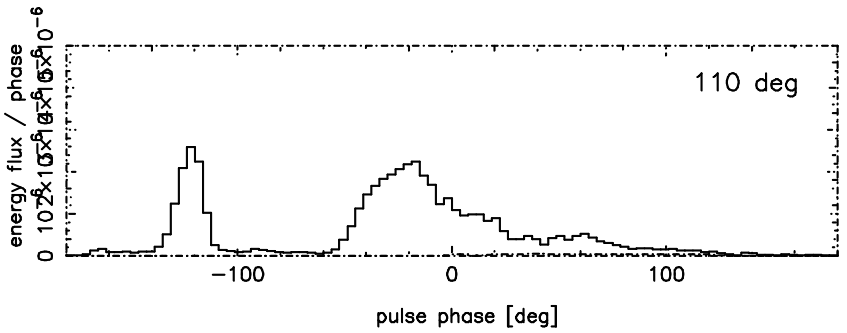


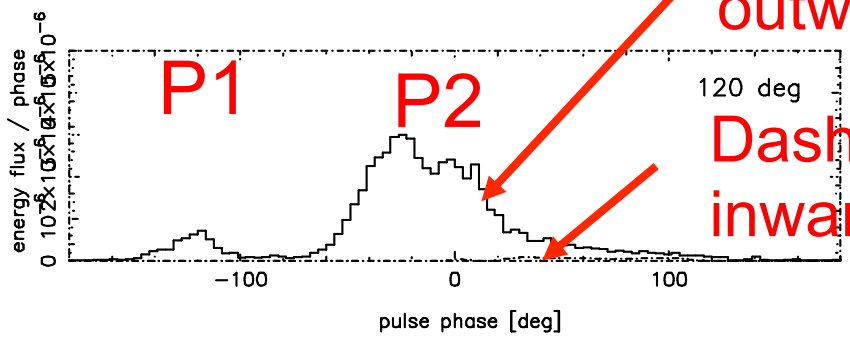


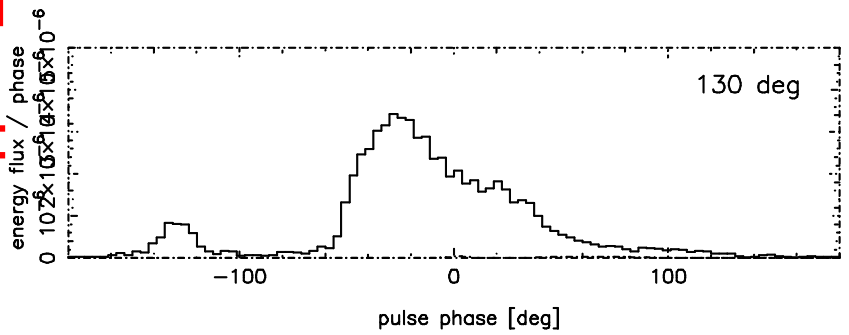


Solid: outward

Dashed: inward

One NS rotation

# §3 Non-vacuum 3-D outer-gap model

Example of SED @ $\zeta=110^{o}$ for $\tau=3$kyr pulsar.

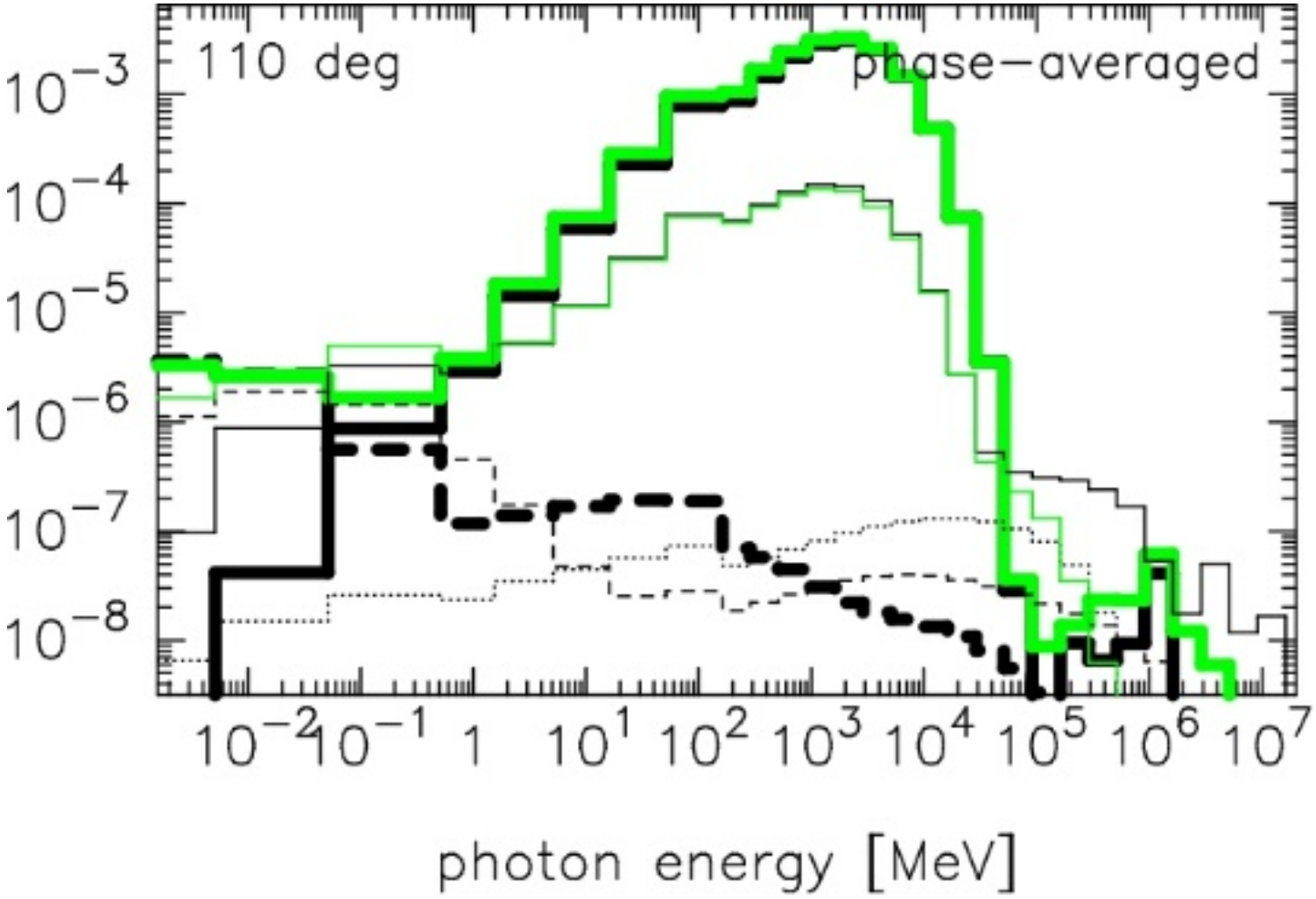

# §4 Discussion

The same method can be applied to BH magnetospheres.

E.g., BH lightning due to particle acceleration @ horizon scale (Science 346, 1080-1084, MAGIC collaboration 2014)

MAGIC observed radio galaxy IC 310 (S0, $z$=0.0189) on November 12-13, 2012. $M$-$\sigma$ rel.→ $M=(1\sim7)\times10^8\,M_\odot$, $\Delta t_{BH}$ = 8~57 min.

An extraordinary outburst was detected above 300 GeV.

A conservative estimate of the shortest variability, $\Delta t_{obs}$=4.8 min < (0.08-0.6)$\Delta t_{BH}$.

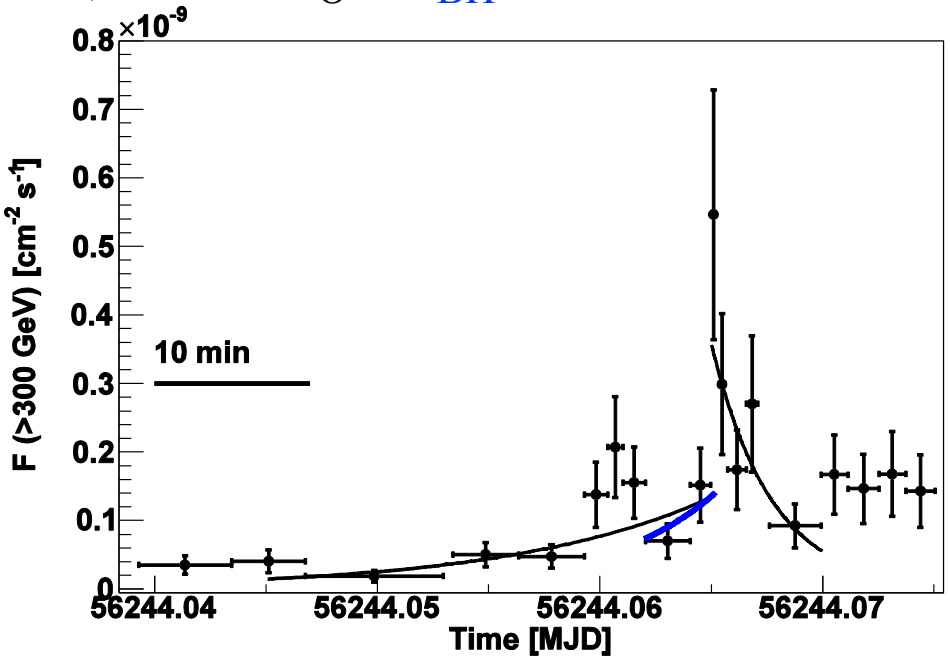

# §4 Discussion

BH lightning due to particle acceleration @ horizon scale

(Science 346, 1080-1084, MAGIC collaboration 2014)

If the initial perturbation originates in the AGN-rest frame, the variability takes place at sub-horizon scale.

Mrk 501 & PKS 2155-304 show VHE variabilities with flux doubling times scales, $\Delta t_{obs} \sim 2$ min « $\Delta t_{BH}$. (~70-80 min.)

(Albert + 2007, ApJ 685, L23; Abramowski + 2012, ApJ 746, 151)

Imagine a perturbation initiating in the AGN-rest frame with variation time scale $\Delta t_{AGN}$.

The perturbation enters into the jet with time scale $\Gamma \Delta t_{AGN}$.

We detect variation $\Delta t_{obs} = (1+z)\ (\Gamma/\delta)\ \Delta t_{AGN} \sim \Delta t_{AGN}$.

Since $\Gamma \sim \delta$, Lorentz factors cancel out in the observer's frame.

Thus, $\Delta t_{obs}$ « $\Delta t_{BH}$ indicates variations at sub-horizon scales.

# §4 Discussion

## BH lightning due to particle acceleration @ horizon scale

(Science 346, 1080-1084, MAGIC collaboration 2014)

They proposed the Magnetospheric particle acceleration model (e.g., Levinson 2011, ApJ 730, 123).

In a charge-starved magnetosphere, $E_{||}$, arises along the ***B*** line.

In AD corona, $e^{\pm}$'s are supplied via thermal γγ pair production. At very low accretion rate, charge depletion leads to a sub-Goldreich-Julian density,

$$n_{e^{\pm}}/n_{GJ} = 0.02 \dot{m}^{-4} M_8^{0.5} .$$

Thus, provided that the radiation is inefficient in the AD, the force-free approximation breaks down and a vacuum gap is formed. The radiation will be highly beamed along the local ***B*** lines.

# §4 Discussion

## BH lightning due to particle acceleration @ horizon scale

(Science 346, 1080-1084, MAGIC collaboration 2014)

They proposed the Magnetospheric particle acceleration model (e.g., Levinson 2011, ApJ 730, 123).

In another word, by analogy with the pulsar outer-gap model, $E_{||}$ arises around the null-charge surface, where $\rho_{GJ}$ vanishes.

(Their argument, which is not very trivial.)

- The intermittent variability of IC 310 is due to a runaway effect.
- As particles accelerate to ultrahigh energies, EM cascades develop to provide charges until their current shortcuts the gap.
- The excess particles are then swept away with the jet flow, until the gap reappears.
- Cascaded pairs efficiently screen $E_{||}$ to terminate the flare. Thus, the emission may take place like lightning.

# §4 Discussion

The BH outer-gap model (Science 346, 1080-1084, MAGIC collaboration 2014; Levinson 2011, ApJ 730, 123) can be quantified very easily.

It was initially proposed by Beskin (1992, Soviet Astron., 36(6), 642) and quantified by KH & Okamoto.

KH & Okamoto 1998, ApJ 497, 563

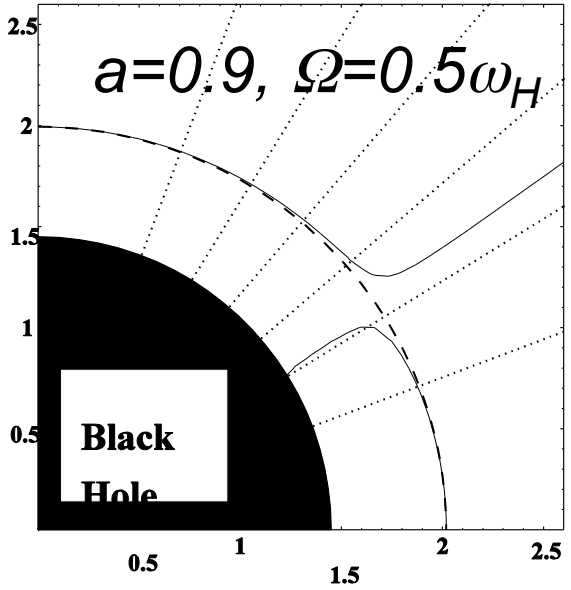


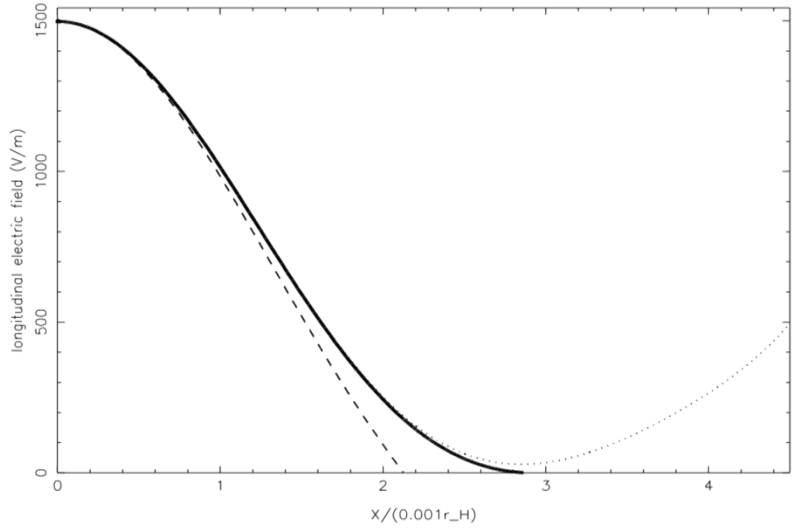


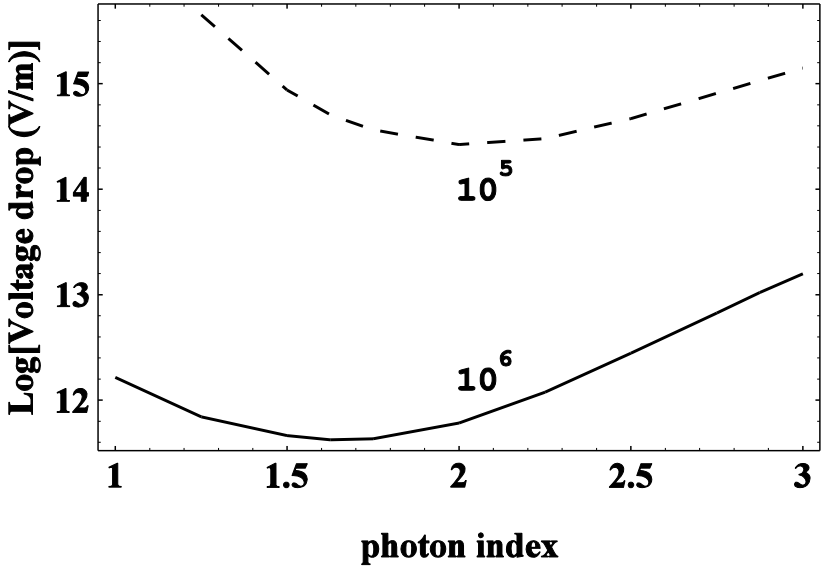

# *Summary*

- OG model is one of the promising models in HE/VHE emission models from pulsar & BH magnetospheres.
- We can predict the HE/VHE emissions from OGs, by solving the set of Maxwell ($\mathrm{div}\boldsymbol{E}=4\pi\rho$) and $e^{\pm}$ Boltzmann eqs., radiative transfer eq., if we specify $P$, $dP/dt$, $\alpha_{\mathrm{incl}}$, $kT_{\mathrm{NS}}$.
- The solution corresponds to a quantitative extension of classic outer gap model. We no longer have to assume the gap geometry, $E_{\parallel}$, $e^{\pm}$ distribution functions.
- To obtain the observed double peak light curve, the photon flux should be predominantly outward in an OG.
- The non-vacuum 3D OG model naturally reproduces predominantly outward γ-ray flux.